HEPHY-PUB--566-91.

HEPHYPUB-1991-566
(UWThPh-1991-60)

AT9200026

Production and Decay of Supersymmetric Particles at Future Colliders

A. Bartl
Institut für Theoretische Physik
Universität Wien, A-1090 Vienna

W. Majerotto and B. Mößlacher
Institut für Hochenergiephysik
Österreichische Akademie der Wissenschaften, A-1050 Vienna

1 Introduction

Despite its impressive success it is generally believed that the Standard Model is still not the final theory of fundamental particle interactions. At present, one of the most attractive possibilities of extending the Standard Model is provided by supersymmetry (SUSY). A supersymmetric extension of the Standard Model allows us to incorporate in a natural way elementary scalar particles such as the Higgs boson into a quantum field theoretical framework. Moreover, it may enable us to relate the weak symmetry breaking scale to the grand unification scale [1, 2, 3].

If these ideas about 'low-energy' supersymmetry are true, one expects the supersymmetric particles to have masses below or about 1 TeV. The possibility that some of the SUSY particles may have masses even much lower than this value has tremendously stimulated the interest in experimental searches at the present accelerators (CERN-S$p\bar{p}$S-Collider, FNAL-Tevatron, TRISTAN, LEP100). The search for supersymmetry will also play an important rôle in the future, when experiments at higher energies can be performed.

In this paper we shall describe how supersymmetric particles could be detected at the new colliders HERA, LEP200, LHC, SSC, and at a possible future linear e^+e^- collider. We shall present theoretical predictions for production cross sections and decay probabilities, as well as for the important signatures. Our calculations will be based on the Minimal Supersymmetric Standard Model (MSSM) which is the simplest supersymmetric extension of the Standard Model.

Like the Standard Model, the MSSM is based on the $SU(3) \times SU(2) \times U(1)$ gauge symmetry group, spontaneously broken down to $SU(3) \times U(1)_{em}$. It has the minimal particle content, i.e. it contains the known particles, the gauge bosons, quarks and leptons, plus their superpartners, the gauginos $(\tilde{g}, \tilde{W}^{\pm}, \tilde{Z}, \tilde{\gamma})$, squarks $\tilde{q}$ and sleptons $\tilde{\ell}$. As is well known, two Higgs doublets are necessary, $H_1 = (H_1^0, H_1^-)$ and $H_2 = (H_2^+, H_2^0)$, together with their superpartners, the higgsinos $(\tilde{H}_{1,2}^0, \tilde{H}^{\pm})$.

The non-strongly interacting gauginos mix with the higgsinos to form corresponding mass eigenstates. There are two pairs of charginos $\tilde{\chi}_i^\pm$, $i = 1, 2$, and four neutralinos $\tilde{\chi}_i^0$, $i = 1, \ldots, 4$, in order of their mass eigenvalues. The masses and couplings of the charginos and neutralinos are determined by the corresponding mass matrices [2, 4]. These depend on the parameters M, M', μ, and $\tan\beta = v_2/v_1$. M and M' are the $SU(2)$ and $U(1)$ gaugino masses, sometimes also called M_2 (or $m_{1/2}$) and M_1, respectively. μ is the mass parameter introduced in the superpotential term $\mu H_1 H_2$. v_1 and v_2 are the vacuum expectation values of the two Higgs doublets. In the following we shall use the relations $M/m_{\tilde{g}} = (\alpha_2/\alpha_3) \approx 0.3$ and, assuming GUT, $M'/M = (5/3)\tan^2\theta_W \approx 0.5$, where $m_{\tilde{g}}$ is the gluino mass. Without loss of generality we take $M \geq 0$.

To the two chirality states of the charged leptons and quarks correspond the right and left scalar particles $\tilde{\ell}_R$, $\tilde{\ell}_L$ and $\tilde{q}_R$, $\tilde{q}_L$. The masses of the scalar particles follow from renormalization group equations [5]

$$m^2_{\tilde{f}_{L,R}} = m_f^2 + m_0^2 + C(\tilde{f})M^2 \pm m_Z^2 \cos 2\beta (T_3^f - Q^f \sin^2\theta_W) \tag{1.1}$$

where T_3^f and Q^f are the third component of the weak isospin and charge of the corresponding left- or right-handed fermion, m_0 is the common scalar mass at the unification point, and $C(\tilde{\ell}_R) \approx 0.23$, $C(\tilde{\ell}_L) = C(\tilde{\nu}_e) \approx 0.79$, $C(\tilde{q}_L) \approx 10.8$, $C(\tilde{q}_R) \approx 10.1$. Usually, $\tilde{f}_L$ and $\tilde{f}_R$ are to a good approximation also mass eigenstates. An exception may be the scalar top quark where there is $\tilde{t}_L - \tilde{t}_R$ mixing proportional to the large top quark mass.

The MSSM contains five physical Higgs particles: h^0, H^0, $A^0(0^-)$ and $H^\pm$. In lowest order the masses of the Higgs particles are given in terms of two parameters (commonly used m_A and $\tan\beta$), implying the bounds $m_{h^0} \leq m_Z \leq m_{H^0}$, $m_{h^0} \leq m_A \leq m_{H^0}$, $m_{H^\pm} \geq m_W$ [6]. Radiative corrections can change these tree level masses appreciably due to the large top quark mass [7, 8]. It is possible that $m_{h^0} > m_Z$ and/or $m_{h^0} > m_A$.

Moreover, an analysis of the renormalization group equations based on radiative electroweak symmetry breaking suggests $\tan\beta$ to be in the range $1 \lesssim \tan\beta \lesssim m_t/m_b$.

In the MSSM the multiplicative quantum number R-parity is conserved ($R = +1$ for standard model particles including Higgs bosons, $R = -1$ for the supersymmetric particles). This implies that there is a lightest supersymmetric particle (LSP) which is stable and into which all supersymmetric particles eventually decay. A further consequence is that supersymmetric particles can only be produced in pairs. Usually, the lightest neutralino $\tilde{\chi}_1^0$ is assumed to be the LSP.

To summarize, the following four basic parameters are necessary to specify the SUSY particle sector of the MSSM: m_0, M, μ and $\tan\beta$. For the description of the Higgs sector, at least one further parameter is needed (apart from the top quark mass m_t), for which usually m_A is taken. Production cross sections as well as decay rates depend in a characteristic way on these parameters. Here a systematic study of this dependence in the whole parameter space relevant for this energy will be performed.

In Sect. 2 we shortly review the present experimental bounds and give the expectations for SUSY particle production at future colliders. In Sect. 3, 4, and 5 we treat SUSY particle production and decay in e^+e^-, pp, and ep collisions, respectively. Sect. 6 contains a summary. In the Appendix we give formulae for the e^+e^- production cross sections and for the three-body decays of charginos and neutralinos.

2 Present Experimental Bounds and Expectations

For the charged scalar partners of the fermions the LEP experiments have led to the bound $m_{\tilde{f}} \gtrsim 45$ GeV, and similarly for charginos $m_{\tilde{\chi}_1^\pm} \gtrsim 46$ GeV [9]. From the invisible width of the Z^0 one can derive $m_{\tilde{\nu}} \geq 42$ GeV. An analysis [10] of the CDF data, taking into account cascade decays, has given the lower bound $m_{\tilde{g}} \gtrsim 135$ GeV, whereas for squarks the limits $m_{\tilde{q}} \gtrsim 170$ GeV (for $m_{\tilde{g}} < m_{\tilde{q}}$) and $m_{\tilde{q}} \gtrsim 130$ GeV (for $m_{\tilde{q}} < m_{\tilde{g}} \leq 400$ GeV) are obtained, assuming that all squark masses are equal. However, due to $\tilde{t}_L - \tilde{t}_R$ mixing the stop mass could be much smaller, even below 100 GeV [11]. With $M \approx 0.3 m_{\tilde{g}}$ the bound on the gluino mass implies $M \gtrsim 40$ GeV. From this and the negative neutralino searches at the Z^0 one can derive $m_{\tilde{\chi}_1^0} \gtrsim 19$ GeV for the lightest neutralino.

The present experimental bounds on the neutral Higgs particles in the MSSM, including one-loop radiative corrections are $m_h \geq 41$ GeV and $m_A \geq 20$ GeV [9]. At present the experimental data do not restrict $\tan\beta$.

In the LEP energy range ($\sqrt{s} \leq 190$ GeV) charged sleptons and charginos can be observed if their masses are below 90 GeV. The supersymmetry parameter region accessible is very roughly $m_0 \leq 90$ GeV, and $M \lesssim 90$ GeV with $|\mu|$ arbitrary, or $|\mu| \lesssim 90$ GeV with M arbitrary. At the LHC and SSC gluinos and squarks with masses up to around 1 TeV can be detected. This implies that the region $m_0 \lesssim 1$ TeV and $M \lesssim 300$ GeV can be explored.

An e^+e^- collider at $\sqrt{s} = 500$ GeV allows chargino and selectron searches up to a mass of approximately 250 GeV. This yields an accessible parameter region of roughly $m_0 \lesssim 250$ GeV, and $M \lesssim 250$ GeV with $|\mu|$ arbitrary, or $|\mu| \lesssim 250$ GeV with M arbitrary.

3 e^+e^- Collisions

In e^+e^- collisions the following SUSY particle processes are the most important ones and would give direct evidence for supersymmetry:

$$e^+e^- \rightarrow \tilde{\chi}_i^+ + \tilde{\chi}_j^-, \quad i,j = 1,2 \tag{3.1}$$
$$e^+e^- \rightarrow \tilde{\chi}_i^0 + \tilde{\chi}_j^0, \quad i,j = 1,\ldots 4 \tag{3.2}$$
$$e^+e^- \rightarrow \tilde{e}_{L,R}^+ + \tilde{e}_{L,R}^- \tag{3.3}$$
$$e^+e^- \rightarrow \tilde{\mu}_{L,R}^+ + \tilde{\mu}_{L,R}^- \tag{3.4}$$
$$e^+e^- \rightarrow \tilde{\nu} + \bar{\tilde{\nu}} \tag{3.5}$$
$$e^+e^- \rightarrow \tilde{q}_{L,R} + \bar{\tilde{q}}_{L,R}. \tag{3.6}$$

In order to work out suitable signatures it is also necessary to study the decays of these particles.

The three-body decays of charginos and neutralinos are:

$$\tilde{\chi}_i^\pm \rightarrow l^+ + l^- + \tilde{\chi}_k^\pm,\ q + \bar{q} + \tilde{\chi}_k^\pm,\ l^\pm + \overset{(-)}{\nu} + \tilde{\chi}_k^0,\ q + \bar{q}' + \tilde{\chi}_k^0 \tag{3.7}$$
$$\tilde{\chi}_i^0 \rightarrow l^+ + l^- + \tilde{\chi}_k^0,\ q + \bar{q} + \tilde{\chi}_k^0,\ l^\pm + \overset{(-)}{\nu} + \tilde{\chi}_k^\mp,\ q + \bar{q}' + \tilde{\chi}_k^\pm. \tag{3.8}$$

If kinematically allowed, the two-body decays will be the dominant ones:

$$\tilde{\chi}_i^\pm \rightarrow Z^0 + \tilde{\chi}_k^\pm,\ h^0(A^0 \,\mathrm{or}\, H^0) + \tilde{\chi}_k^\pm,\ W^\pm + \tilde{\chi}_k^0,\ H^\pm + \tilde{\chi}_k^0 \tag{3.9}$$
$$\tilde{\chi}_i^0 \rightarrow Z^0 + \tilde{\chi}_k^0,\ W^\pm + \tilde{\chi}_k^\mp,\ h^0(A^0 \,\mathrm{or}\, H^0) + \tilde{\chi}_k^0,\ H^\pm + \tilde{\chi}_k^\mp. \tag{3.10}$$

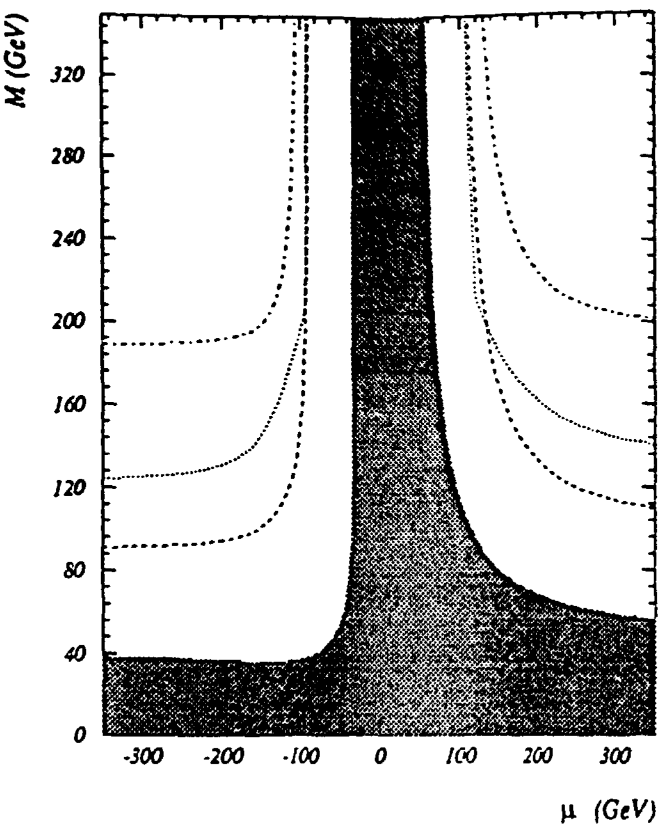

Fig. 1: Parameter region of M, μ, for $\tan\beta = 4$, explorable at LEP200 by chargino and neutralino searches. Shown are border lines for: $\tilde{\chi}^0_1\tilde{\chi}^0_1$ (– · – · –), $\tilde{\chi}^0_1\tilde{\chi}^0_2$ (· · · · ·), $\tilde{\chi}^+_1\tilde{\chi}^-_1$ (– – –) production at $\sqrt{s} = 190$ GeV. Also shown is the region excluded by chargino searches at the Z^0.

The produced sfermions $\tilde{f}_{L,R}$ (slepton or squark) decay into a fermion f (lepton or quark) and a neutralino $\tilde{\chi}^0_i$ or chargino $\tilde{\chi}^{\pm}_i$:

$$\tilde{e}_{L,R} \rightarrow e + \tilde{\chi}^0_i,\ \tilde{e}_L \rightarrow \nu + \tilde{\chi}^-_i \tag{3.11}$$

$$\tilde{\nu}_L \rightarrow \nu + \tilde{\chi}^0_i,\ e^- + \tilde{\chi}^+_i \tag{3.12}$$

$$\tilde{q}_{L,R} \rightarrow q + \tilde{\chi}^0_i, \tilde{q}_L \rightarrow q' + \tilde{\chi}^{\pm}_i,\ \tilde{u}_L \rightarrow d + \tilde{\chi}^+_i,\ \tilde{d}_L \rightarrow u + \tilde{\chi}^-_i. \tag{3.13}$$

In this section we consider only squarks corresponding to light quark flavours. If the gluino is lighter than the squark, then the squark would first decay into a gluino:

$$\tilde{q}_{L,R} \rightarrow q + \tilde{g}. \tag{3.14}$$

As the lightest neutralino $\tilde{\chi}^0_1$ is supposed to be the LSP, all SUSY particles will eventually decay into $\tilde{\chi}^0_1$. At high energies and masses in general cascade decays of SUSY particles occur leading to a rather complex decay pattern. This has a strong influence on the experimental signature of SUSY particles, in particular on the classical 'missing energy' signature. (In the following missing momentum will be denoted by $\not{p}$.) According to eqs. (3.9) and (3.10) some of the SUSY particles may also decay into Higgs particles. Therefore, the actual masses and couplings of the Higgs particles will influence some of the signatures. As is well known radiative corrections may appreciably change the Higgs masses compared with their tree level values [7, 8].

The formulae for the various cross sections and decays have been worked out by several authors, see [12], where a rather complete list of references is given. In the Appendix we present the formulae for the cross sections of the reactions (3.1 – 3.6), and for the three-body decays (3.7) and (3.8). The formulae for the two-body decays (3.9) and (3.10) can be found in [12, 13], and for the sfermion decays (3.11 – 3.13) in [12].

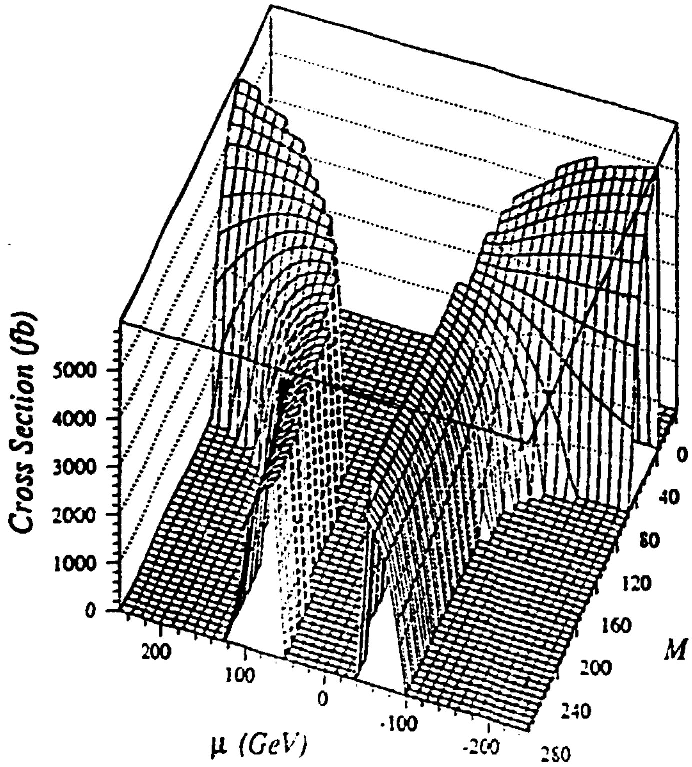

Fig. 2: Cross section for $e^+e^- \to \tilde{\chi}_1^+\tilde{\chi}_1^-$, as a function of M and μ, for $\sqrt{s} = 190$ GeV, $m_{\tilde{\nu}} = 300$ GeV, $\tan\beta = 4$.

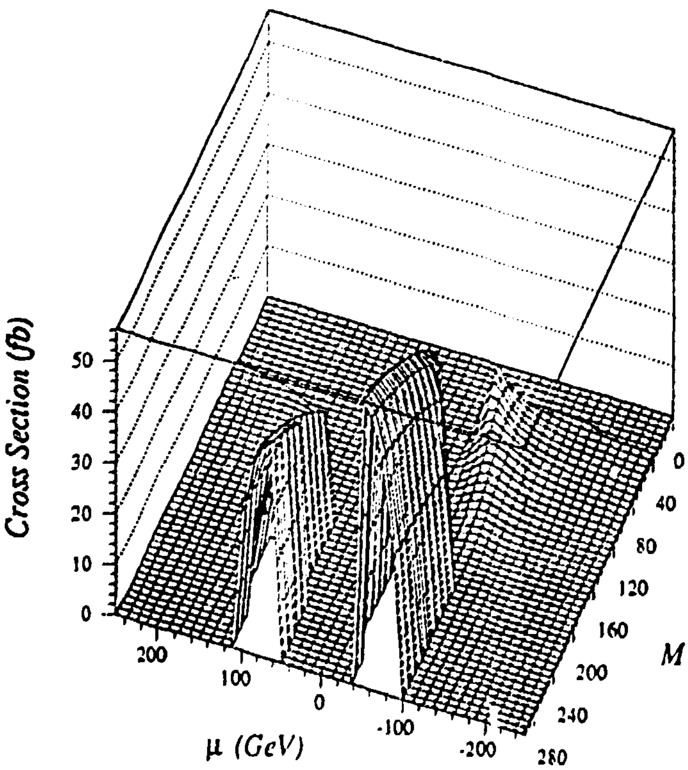

Fig. 3: Cross section for $e^+e^- \to \tilde{\chi}_1^0\tilde{\chi}_2^0 \to (e^+e^-) + \not{p}$ (one-sided), as a function of M and μ, for $\sqrt{s} = 190$ GeV, $m_{\tilde{e}} = m_{\tilde{\nu}} = m_{\tilde{q}} = 300$ GeV, $\tan\beta = 4$.

3.1 LEP 200

The predictions for cross sections will be given for $\sqrt{s} = 190$ GeV, assuming an integrated luminosity of 500 pb^{-1} per year. For earlier studies we refer to [14].

3.1.1 Chargino production

In Fig. 1 we show the region in the (M, μ) plane (for $\tan\beta = 4$) which can be explored at LEP200 by searching for charginos and neutralinos. The region already excluded by unsuccessful search at the Z^0 is also indicated. For other values of $\tan\beta$ similar plots are obtained.

The production mechanism for $e^+e^- \to \tilde{\chi}_i^+ + \tilde{\chi}_j^-$, $i,j = 1,2$, is γ, Z exchange in the s channel and $\tilde{\nu}$ exchange in the t channel. The total production cross section for $e^+e^- \to \tilde{\chi}_1^+ + \tilde{\chi}_1^-$ is shown in Fig. 2 for $m_{\tilde{\nu}} = 300$ GeV and $\tan\beta = 4$. It can reach 6 fb. If both $M \gtrsim 90$ GeV and $|\mu| \gtrsim 90$ GeV, the light chargino becomes too heavy to be produced at this energy. If $|\mu| > M$ then $\tilde{\chi}_1^+$ is more gaugino-like, and if $M > |\mu|$ it is more higgsino-like. Therefore, sneutrino exchange can have a substantial influence for $|\mu| > M$, especially if $m_{\tilde{\nu}} \simeq m_Z$. The $\tan\beta$ dependence is in general weak.

The decay of the chargino, $\tilde{\chi}_1^+ \to \tilde{\chi}_1^0 + l + \nu$, $\tilde{\chi}_1^0 + q + \bar{q}$, lead to 'two sided' events with acollinear, acoplanar hard leptons or jets and large missing energy: $l^+ + l^- + \not{p}$ or $l^\pm +$ jets $+ \not{p}$ or jets $+$ jets $+ \not{p}$. For $m_{\tilde{e}} = m_{\tilde{\nu}} = m_{\tilde{q}} = 300$ GeV and $\tan\beta = 4$ we obtain for these signatures a rate of 0.07 pb, 0.5 pb, 3.5 pb, respectively.

A priori, it cannot be excluded that the sneutrino and/or the left slepton $\tilde{l}_L$ are lighter than the chargino. In this unlikely case the chargino would first decay into $\tilde{\nu}$ or $\tilde{l}_L$. This would drastically enhance the leptonic signal.

A recent detailed study of chargino production at LEP200 is given in [15].

3.1.2 Neutralino production

As can be seen in Fig. 1 the SUSY parameter region for the reaction $e^+e^- \to \tilde{\chi}_1^0\tilde{\chi}_2^0$ is larger than that for chargino production. Here the reaction mechanism is Z exchange in the s channel and $\tilde{e}_{L,R}$ exchange in the t and u channel. The Z^0 couples only to the Higgsino components of the neutralinos, whereas the selectron couples only to the gaugino-component. For $M < |\mu|$ the $\tilde{\chi}_1^0$ is gaugino-like, whereas for $M > |\mu|$ it has large higgsino-components. Therefore, one expects sufficiently large cross sections for $M > |\mu|$. Only if $m_{\tilde{e}} \simeq m_Z$ we get sizeable cross sections also in the region $M < |\mu|$. The total cross section can go up to 1.7 pb (for $m_{\tilde{e}} = 300$ GeV).

The $\tilde{\chi}_2^0$ has the following decay modes: $\tilde{\chi}_2^0 \to \tilde{\chi}_1^0 f\bar{f}$, and $\chi_1^\pm f\bar{f}'$ if kinematically allowed. This leads to one-sided events. In Fig. 3 we show the cross section for $e^+e^- \to \tilde{\chi}_1^0\tilde{\chi}_2^0 \to (e^+e^-) + \not{p}$ as a function of M and μ, for $m_{\tilde{e}} = m_{\tilde{\nu}} = m_{\tilde{q}} = 300$ GeV and $\tan\beta = 4$. The cross section for $e^+e^- \to \tilde{\chi}_1^0\tilde{\chi}_2^0 \to$ (jet jet $+ \not{p}$ is approximately a factor 20 higher and can reach 1.3 pb.

If the sneutrino is lighter than the $\tilde{\chi}_2^0$, and the $\tilde{\chi}_2^0$ has a non-vanishing Z-ino component, then the decay $\tilde{\chi}_2^0 \to \tilde{\nu} + \bar{\nu}$ would dominate, where the sneutrino is invisible. Then the $\tilde{\chi}_2^0$ would be produced undetectably.

In the case of a light slepton, $m_{\tilde{l}} < m_{\tilde{\chi}_2^0}$, the $\tilde{\chi}_2^0$ would first decay into $\tilde{l}^\pm + l^\mp$, yielding strongly enhanced leptonic rates.

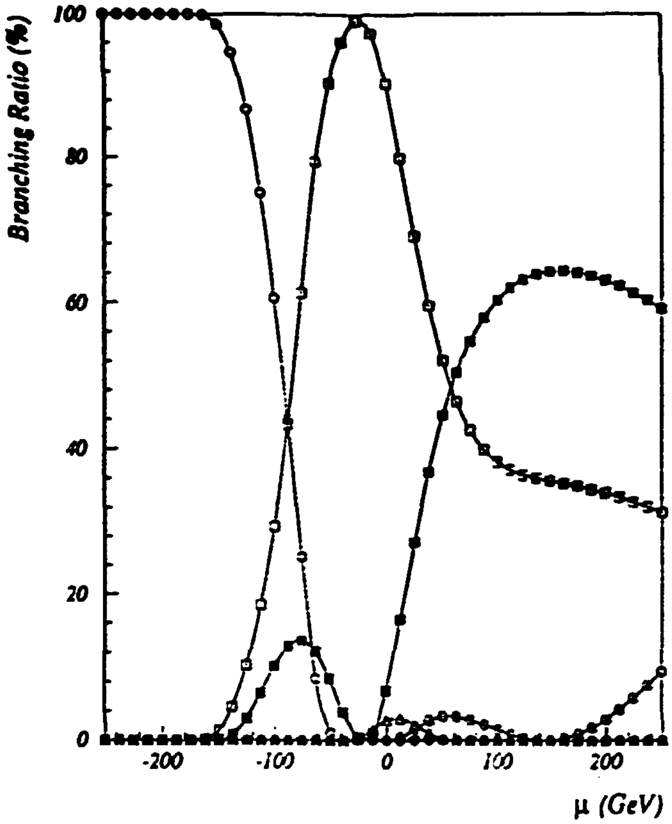

Fig. 4: Branching ratios for $\tilde{e}_L$ decays into charginos and neutralinos, as a function of μ, for $m_{\tilde{e}_{L,R}} = 80$ GeV, $M = 80$ GeV, $\tan\beta = 4$, $\sin^2\theta_W = 0.23$. The curves correspond to the following transitions:

- ■ into the light chargino $\tilde{\chi}_1^{\pm}$
- ● into the heavy chargino $\tilde{\chi}_2^{\pm}$
- o into $\tilde{\chi}_1^0$
- □ into $\tilde{\chi}_2^0$
- △ into $\tilde{\chi}_3^0$

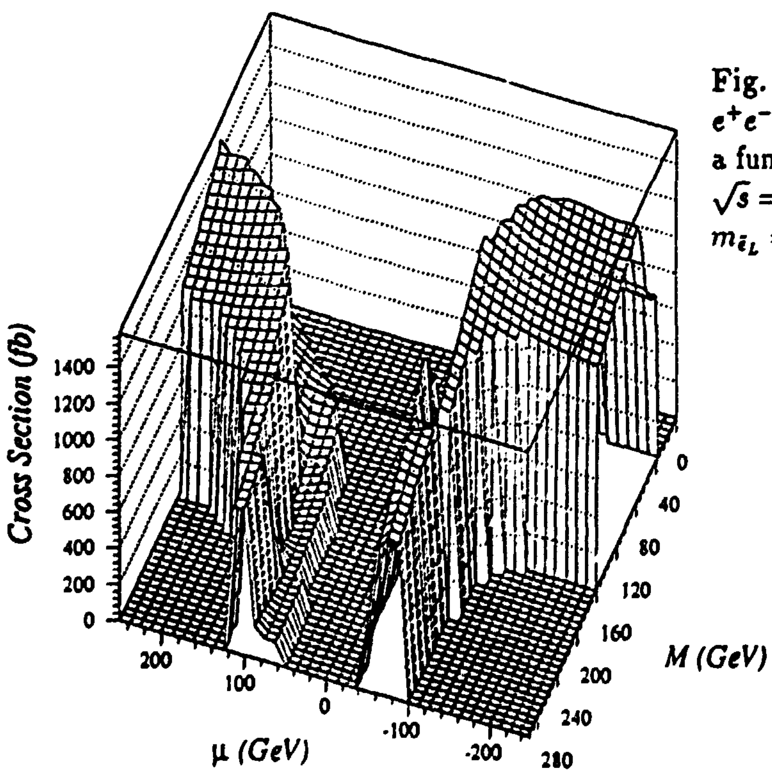

Fig. 5: Cross section for $e^+e^- \to \tilde{e}_{L,R} + \tilde{e}_{L,R} \to e^+e^- + \not{p}$, as a function of M and μ, for $\sqrt{s} = 190$ GeV, $m_{\tilde{e}_L} = m_{\tilde{e}_R} = 80$ GeV, $\tan\beta = 4$.

3.1.3 Selectron production

Here the reactions $e^+e^- \to \tilde{e}_R^+ + \tilde{e}_R^-, \tilde{e}_L^+ + \tilde{e}_L^-, \tilde{e}_L^\pm + \tilde{e}_R^\mp$ can occur. The reaction mechanism for selectron pair production $e^+e^- \to \tilde{e}_L^+ + \tilde{e}_L^-, \tilde{e}_R^+ + \tilde{e}_R^-$, is (γ, Z) exchange in the s channel and $\tilde{\chi}_i^0$ exchange in the t channel. The process $e^+e^- \to \tilde{e}_L^\pm + \tilde{e}_R^\mp$ receives only t-channel contributions.

The total cross section $\sigma(\tilde{e}_L\tilde{e}_L + \tilde{e}_R\tilde{e}_R + 2(\tilde{e}_L\tilde{e}_R))$ varies between 0.75 and 1.75 pb for $m_{\tilde{e}} = 80$ GeV, depending mainly on the SUSY parameter M and only weakly on μ and $\tan\beta$.

$\tilde{e}_L$ and $\tilde{e}_R$ decay differently: $\tilde{e}_L \to e\tilde{\chi}_1^0, e\tilde{\chi}_2^0, \nu\tilde{\chi}_1^-$, $\tilde{e}_R \to e\tilde{\chi}_1^0, e\tilde{\chi}_2^0$, where $\tilde{\chi}_2^0$ and $\tilde{\chi}_1^-$ further decay until $\tilde{\chi}_1^0$ is produced. The decay pattern of $\tilde{e}_R$ is simpler because the direct decay into the LSP dominates. For illustration we show in Fig. 4 the branching ratios for $\tilde{e}_L$ decays as a function of μ for $m_{\tilde{e}_L} = 80$ GeV, $M = 80$ GeV, $\tan\beta = 4$. As can be seen, cascade decays are possible if approximately $M < m_{\tilde{e}_L}$ or $|\mu| < m_{\tilde{e}_L}$.

In Fig. 5 we show the cross section for the 'classical' signature $e^+e^- \to e^+ + e^- + \not{p}$, as a function of M and μ, for $m_{\tilde{e}} = 80$ GeV, $\tan\beta = 4$. Notice that the parameter region covered by LEP at the Z^0 is left out. The region $|\mu| \gtrsim 120$ GeV for $M \gtrsim 160$ GeV is excluded because the selectron would be heavier than the LSP. The cross section for this signature can reach a value of 1.5 pb. It can also be seen that the rate is much smaller where cascade decays are possible.

In $e^+e^- \to \tilde{\mu}_{L,R}^+\tilde{\mu}_{L,R}^-$ there is only (Z,γ) exchange. Hence the total cross section is smaller, $\sigma = 0.19$ pb for $m_{\tilde{\mu}} = 80$ GeV.

3.1.4 Sneutrino Production

In the MSSM there is only a left-sneutrino $\tilde{\nu} \equiv \tilde{\nu}_L$. The reaction $e^+e^- \to \tilde{\nu}_e + \bar{\tilde{\nu}}_e$ has contributions from Z^0 exchange in the s channel and $\tilde{\chi}_i^\pm$ exchange in the t channel.

The total cross section can go up to 3 pb for $m_{\tilde{\nu}} = 80$ GeV. The sneutrino can, however, only be seen if it decays in a cascade, $\tilde{\nu} \to e^-\tilde{\chi}_1^+ \to e^-\tilde{\chi}_1^0 f\bar{f}'$, or $\tilde{\nu} \to \nu\tilde{\chi}_2^0 \to \nu\tilde{\chi}_1^0 f\bar{f}$, because the direct decay into the LSP, $\tilde{\nu} \to \nu\tilde{\chi}_1^0$, is invisible. Such visible decays can occur only if $M < m_{\tilde{\nu}_e}$ or $|\mu| < m_{\tilde{\nu}_e}$. Possible signatures are the one-sided events: e^+e^- (or $e^-\mu^+$) $+ \not{p}$, e^-jets $+ \not{p}$, jets $+ \not{p}$, and the two-sided events: (e jets) + (e jets) $+ \not{p}$, etc. Fig. 6 shows the rate for $e^+e^- \to \tilde{\nu}\bar{\tilde{\nu}} \to (e^+e^-) + \not{p}$ (one-sided), as a function of M and μ, for $m_{\tilde{\nu}} = 80$ GeV und $\tan\beta = 4$. The cross section for $e^+e^- \to \tilde{\nu}\bar{\tilde{\nu}} \to$ (e jet $+ \not{p}$ is roughly a factor of 7 higher.

3.2 e^+e^- collisions at 500 GeV

It is conceivable that SUSY particles only show up at energies of several 100 GeV. In this case an e^+e^- collider with an energy well above 200 GeV would be well suited to test the idea of supersymmetry. Presently, several options for a linear e^+e^- collider in the energy range $\sqrt{s} = 0.5 - 2$ TeV are being discussed [16]. Most recently, detailed studies on the physics potential of such a collider at $\sqrt{s} = 500$ GeV were performed [17]. This step in energy would considerably enlarge the explorable parameter range. Experiments at such a collider would allow a crucial test of the MSSM. In particular, if no Higgs particles were found, the MSSM would be ruled out [18]. It is therefore appropriate to study the SUSY particle production reactions (3.1 - 3.6) and the decays of these particles also at this energy. A detailed study is given in [19]. A new feature is that also the higher mass states of the charginos and the neutralinos may be accessible, and cascade decays play a

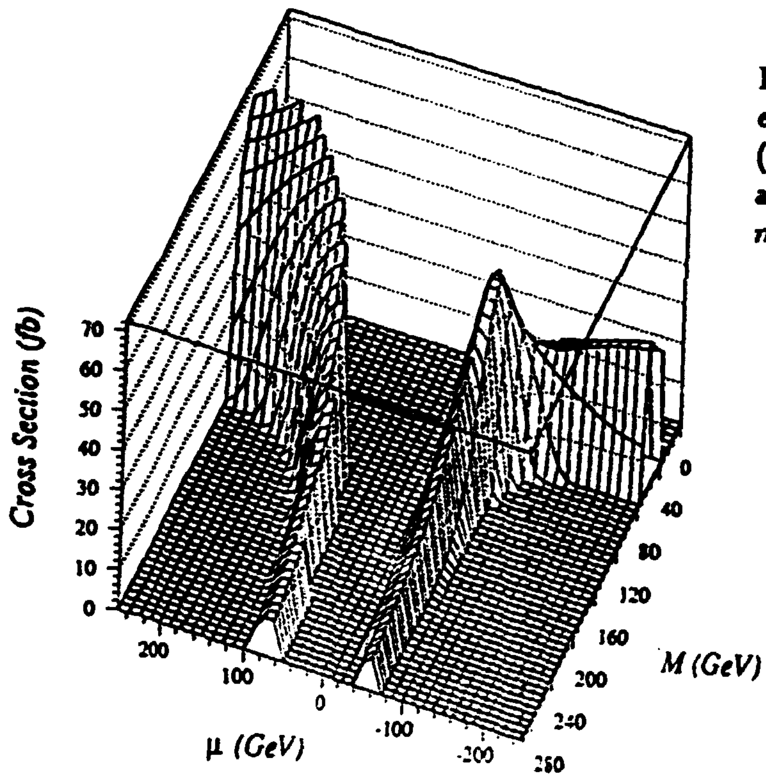

Fig. 6: Cross section for $e^+e^- \to \tilde{\nu}\tilde{\nu} \to (e^+e^-) + \not{p}$ (one-sided), as a function of M and μ, for $\sqrt{s} = 190$ GeV, $m_{\tilde{\nu}} = 80$ GeV and $\tan\beta = 4$.

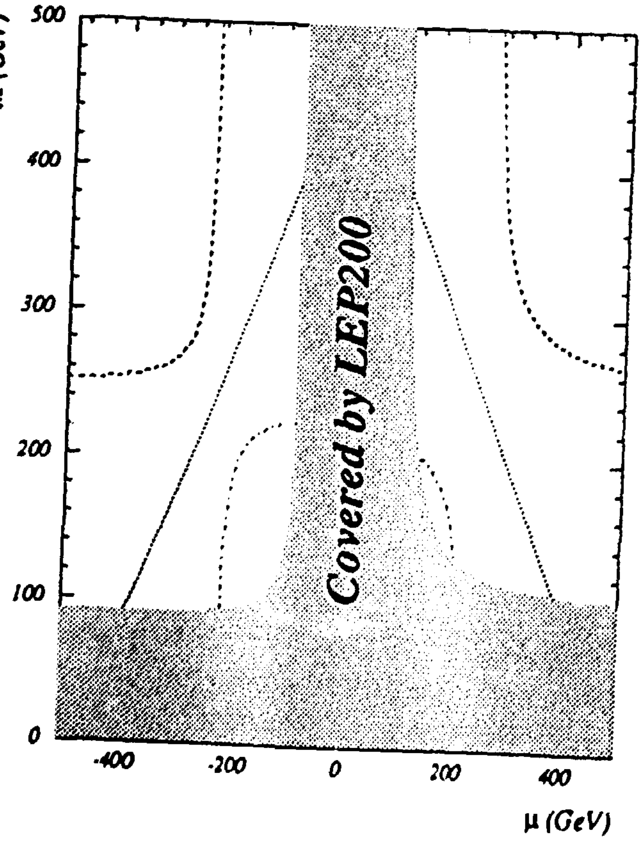

Fig. 7: Supersymmetry parameter space (M, μ) for chargino production at $\sqrt{s} = 500$ GeV, $\tan\beta = 4$. Shown are borderlines for $e^+e^- \to \tilde{\chi}_1^+ + \tilde{\chi}_1^-$ (- - -), $e^+e^- \to \tilde{\chi}_1^\pm + \tilde{\chi}_2^\mp$ (· · ·), $e^+e^- \to \tilde{\chi}_2^+ + \tilde{\chi}_2^-$ (- · - · -). Also shown the region explored by LEP200.

more important rôle than at lower energies. For the following predictions of event rates we shall assume an integrated luminosity of 20 fb^{-1} per year.

A study of SUSY particle production in e^+e^- collisions at $\sqrt{s} = 2$ TeV is given in [12].

3.2.1 Chargino production

Besides the pair production of the lightest chargino, $e^+e^- \to \tilde{\chi}_1^+\tilde{\chi}_1^-$, also the reactions $e^+e^- \to \tilde{\chi}_1^\pm\tilde{\chi}_2^\mp$ and $e^+e^- \to \tilde{\chi}_2^+\tilde{\chi}_2^-$ are possible. The parameter region in the (M,μ) plane (for $\tan\beta = 4$) accessible by these reactions is shown in Fig. 7. Notice that the contour lines $m_{\tilde{\chi}_1^\pm} + m_{\tilde{\chi}_2^\pm}$ = const are straight lines in the (M,μ) plane. If $M > |\mu|$, then $\tilde{\chi}_1^\pm$ is more higgsino-like and $\tilde{\chi}_2^\pm$ more wino-like, and vice versa for $M < |\mu|$. The chargino masses are approximately M and $|\mu|$.

In Fig. 8 we show the total cross section as a function of M and μ for $\sqrt{s} = 500$ GeV, $\tan\beta = 4$, $m_{\tilde{\nu}} = 600$ GeV. The cross section can go up to 550 fb. If both $M \gtrsim 250$ GeV and $|\mu| \gtrsim 250$ GeV the light chargino becomes too heavy to be produced at this energy. It should be noted that for $M \lesssim 250$ GeV there is a dependence on the sneutrino mass. The cross section is smaller by 50 % for $m_{\tilde{\nu}} = 100$ GeV than for $m_{\tilde{\nu}} = 600$ GeV. This can be explained by a destructive interference between the Z and $\tilde{\nu}$ exchange and because the $\tilde{\nu}$ couples only to the gaugino component of the chargino which is dominant for $M \leq |\mu|$. The $\tan\beta$ dependence is in general weak.

In a restricted range of parameters the chargino $\tilde{\chi}_1^\pm$ can also decay first into $\tilde{\chi}_2^0$ (see eq. (3.7)) , although the direct decay into $\tilde{\chi}_1^0$ is still the dominant one. In a certain region of parameters the $\tilde{\chi}_1^\pm$ can decay into real $W^\pm$'s, $\tilde{\chi}_1^\pm \to \tilde{\chi}_1^0 + W^\pm$.

The signatures are 'two-sided' events with acollinear, acoplanar, hard leptons or jets and large missing energy. The rate for $e^+e^- \to \tilde{\chi}_1^+\tilde{\chi}_1^- \to e^+ + e^- + \not{p}$ can go up to 7 fb (for $m_{\tilde{\nu}} = m_{\tilde{e}} = m_{\tilde{q}} = 600$ GeV, $\tan\beta = 4$) leading to 140 events/year, assuming an integrated luminosity of 20 fb^{-1}. The rates for the other signatures, $e^+e^- \to \tilde{\chi}_1^+ + \tilde{\chi}_1^- \to e + \text{jets} + \not{p}$ and $e^+e^- \to \tilde{\chi}_1^+ + \tilde{\chi}_1^- \to \text{jets} + \text{jets} + \not{p}$ are larger than the rate for electrons by approximately a factor 14 and 50, respectively, if the masses of the exchanged scalar particles are much larger than m_W. If they are around m_W, then these ratios are different for $M \leq 250$ GeV.

In the case that the sneutrino and/or the left-slepton are lighter than the chargino, the leptonic decay rates would again be strongly enhanced.

A Monte Carlo study of $e^+e^- \to \tilde{\chi}_1^+\tilde{\chi}_1^-$ taking into account beamstrahlung, background processes, and detector simulation, has been performed in [20]. The most severe Standard Model background is $W^\pm$ pair production, which can be reduced by appropriate cuts.

We now discuss the production of a heavy chargino, $e^+e^- \to \tilde{\chi}_1^\pm + \tilde{\chi}_2^\mp$. The production cross section is shown in Fig. 9 as a function of M and μ, for $\tan\beta = 4$, and $m_{\tilde{\nu}} = 600$ GeV. It can go up to 50 fb. The heavy chargino may have quite a complex decay pattern because in general it decays in cascades until the LSP is produced. Two-body decays into real $W^\pm$'s, Z's, and Higgs particles, eq. (3.9), are possible in a large region of parameter space. The $\tilde{\chi}_k^0$ and $\tilde{\chi}_1^\pm$ then further decay. An interesting signature is therefore given by $e^+e^- \to \tilde{\chi}_1^\pm\tilde{\chi}_2^\mp \to Z + X$. The corresponding rate can reach a value of 20 fb yielding 400 events per year. However, this rate depends more sensititvely on the SUSY parameters, especially on the masses of the Higgs particles.

In a smaller region of the parameter space (see Fig. 7) pair production of the heavy chargino is possible, $e^+e^- \to \tilde{\chi}_2^+ + \tilde{\chi}_2^-$. Characteristic signatures would be given by the decays of $\tilde{\chi}_2^\pm$ into real W's and Z's, $e^+e^- \to \tilde{\chi}_2^+\tilde{\chi}_2^- \to Z + Z + X$, $Z + W^\pm + X$, $W^+ + W^- + X$.

M

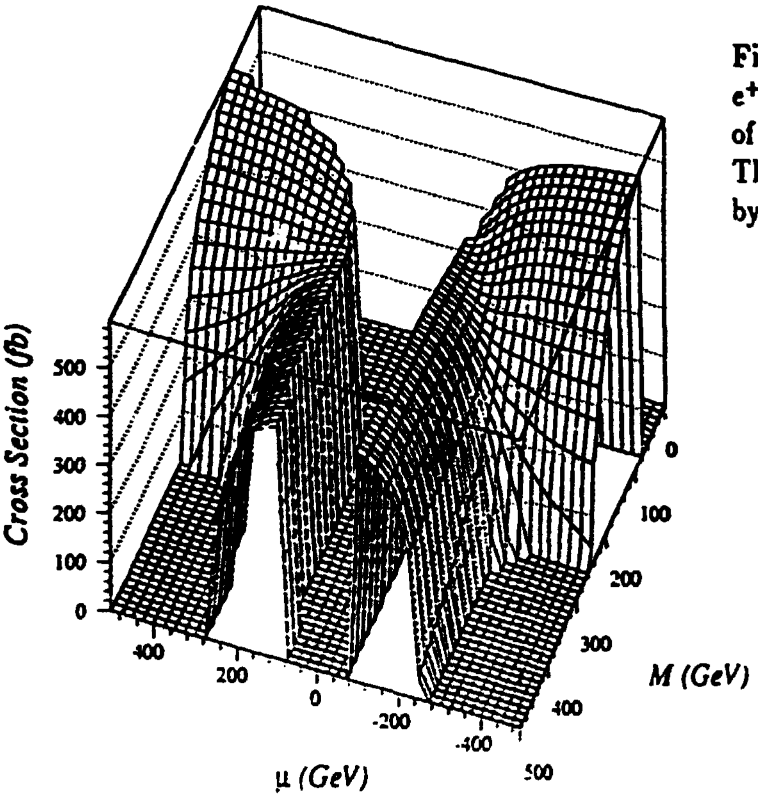

Fig. 8: Total cross section for $e^+e^- \to \tilde{\chi}_1^+ + \tilde{\chi}_1^-$ as a function of M and μ, for $m_{\tilde{\nu}} = 600$ GeV. The parameter region explored by LEP200 is cut out.

3.2.2 Neutralino production

At $\sqrt{s} = 500$ also higher neutralino states can be produced, $e^+e^- \to \tilde{\chi}_i^0 + \tilde{\chi}_j^0$. The parameter region in the (M, μ) plane accessible by the reaction $e^+e^- \to \tilde{\chi}_1^0\tilde{\chi}_2^0$ is again larger than that by $e^+e^- \to \tilde{\chi}_i^+\tilde{\chi}_1^-$. If $m_Z < M < |\mu|$, then $\tilde{\chi}_1^0$ is approximately $\tilde{B}$-ino-like, $\tilde{\chi}_2^0$ is W^3-ino-like, whereas $\tilde{\chi}_3^0$ and $\tilde{\chi}_4^0$ are higgsino-like. On the other hand, if $M > |\mu| > m_Z$, $\tilde{\chi}_1^0$ and $\tilde{\chi}_2^0$ have large higgsino components, whereas $\tilde{\chi}_3^0$ and $\tilde{\chi}_4^0$ are B-ino and W^3-ino-like, respectively. The neutralino masses are approximately $M/2$, M, $|\mu|$, and $|\mu|$ [13, 21].

In the paramter domain also accessible for pair production of light charginos, the cross section for $e^+e^- \to \tilde{\chi}_1^0\tilde{\chi}_2^0$ can go up to 200 fb (for $m_{\tilde{e}} = 600$ GeV). Outside this domain this cross section is, unfortunately at most a few fb, unless the mass of the exchanged selectron is very small (~ 100 GeV).

Again, the most interesting signatures for $\tilde{\chi}_1^0\tilde{\chi}_2^0$ production are one-sided events. The cross section for $e^+e^- \to \tilde{\chi}_1^0\tilde{\chi}_2^0 \to$ (jet jet + $\not{p}$ can reach 130 fb (for $m_{\tilde{\ell}} = m_{\tilde{q}} = m_{\tilde{\nu}} =$ 600 GeV). The rate for $e^+e^- \to \tilde{\chi}_1^0 + \tilde{\chi}_2^0 \to (e^+e^-) + \not{p}$ would be smaller by a factor of approximately 20.

It turns out that some of the production cross sections for the higher neutralino states are comparable to that of $e^+e^- \to \tilde{\chi}_1^0\tilde{\chi}_2^0$. For the higher neutralino states more decay channels are open, and, therefore, cascade decays are more likely. This will lead to a more complex decay pattern and in general reduce the $\not{p}$ signal. On the other hand, more decays into Z's and $W^{\pm}$'s are possible leading to multileptons and/or multijets in the final state. In addition, the rates will depend more sensitively on the properties of the Higgs sector. For a more detailed discussion we refer to [19].

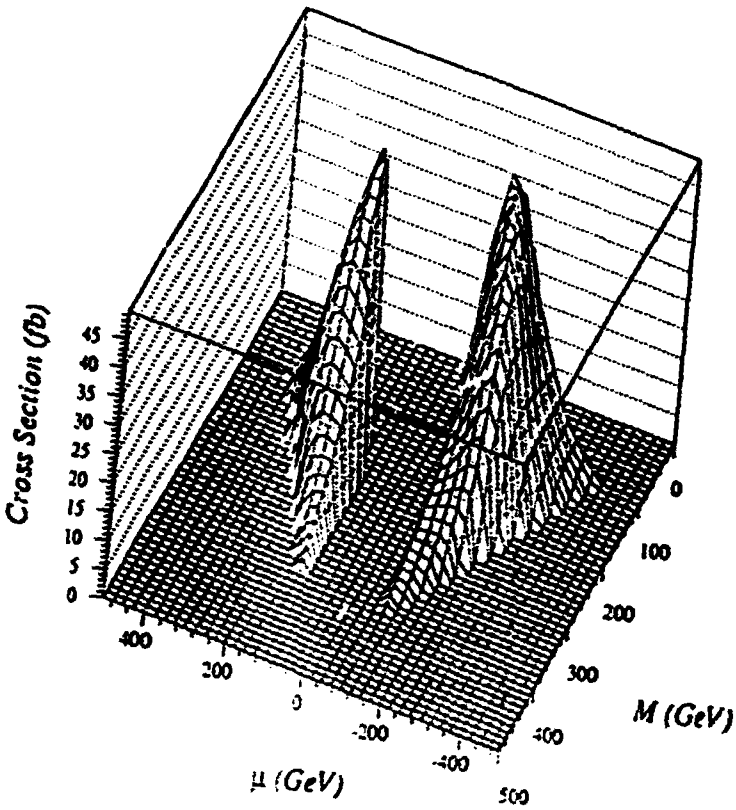

Fig. 9: Total cross section for $e^+e^- \to \tilde{\chi}_1^+ + \tilde{\chi}_2^- + c.c.$ as a function of M and μ for $\tan\beta = 4$, $m_{\tilde{\nu}} = 600$ GeV, $\sqrt{s} = 500$ GeV. The parameter region explored by LEP200 is cut out.

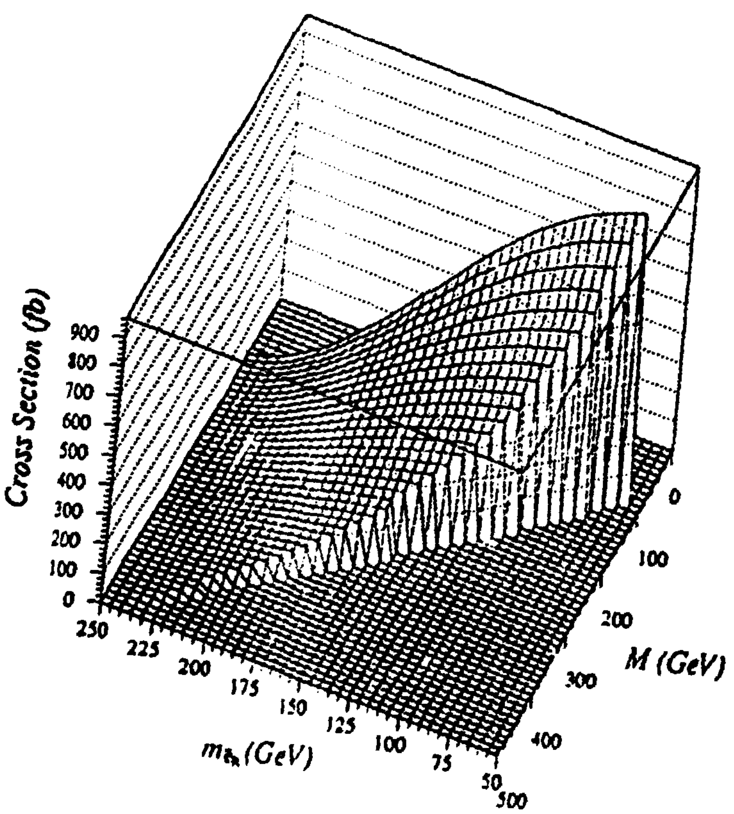

Fig. 10: Total cross section for selectron pair production at $\sqrt{s} = 500$ GeV, $\tan\beta = 4$, $\mu = 200$ GeV $e^+e^- \to \tilde{e}_R^+ + \tilde{e}_R^-$, as a function of M and $m_{\tilde{e}_R}$. The parameter region explored by LEP200 is cut out.

3.2.3 Selectron production

In the energy range considered the mass difference between $\tilde{e}_R$ and $\tilde{e}_L$ according to eq. (1.1) can be quite sizeable. Therefore, in our calculations of selectron production cross sections we shall always use eq. (1.1) to relate $m_{\tilde{e}_R}$ and $m_{\tilde{e}_L}$ to the SUSY arameters m_0, M, $\tan\beta$. Quite generally $\tilde{e}_R$ is lighter than $\tilde{e}_L$.

Since the production cross sections depend only weakly on $\tan\beta$ and μ (apart from the region $|\mu| \lesssim 100$ GeV), we present in Fig. 10 the cross section for $e^+e^- \to \tilde{e}_R^+ + \tilde{e}_R^-$ as a function of M and $m_{\tilde{e}_R}$ for $\mu = -200$ GeV and $\tan\beta = 4$. For $m_{\tilde{e}_R} = 200$ GeV the cross section varies between 50 and 150 fb depending on M. Notice that according to the mass relations, eq. (1.1), there exists a maximal value of M for a given value of $m_{\tilde{e}_L}$ and $m_{\tilde{e}_R}$. It is $M = 410$ GeV for $m_{\tilde{e}_R} = 200$ GeV, and $M = 240$ GeV for $m_{\tilde{e}_L} = 200$ GeV, for $\tan\beta = 4$.

The cross section for $e^+e^- \to \tilde{e}_L^+\tilde{e}_L^-$ is similar in magnitude to that for $\tilde{e}_R\tilde{e}_R$ production. It should be noted that also the cross section for $e^+e^- \to \tilde{e}_L^\pm + \tilde{e}_R^\mp$, which has only t channel contributions, has a comparable cross section, depending on the SUSY parameters.

In the mass region considered, the difference in the decay pattern of $\tilde{e}_R$ and $\tilde{e}_L$ is more pronounced, and cascade decays are expected to play a more important rôle. We show in Figs. 11a and b the branching ratios for the $\tilde{e}_R$ and $\tilde{e}_L$ decays into neutralinos and charginos, eq. (3.11), as function of μ for $M = 150$ GeV, $\tan\beta = 4$, for $m_{\tilde{e}_R} = 200$ GeV and $m_{\tilde{e}_L} = 200$ GeV.

It is noticeable that in a large region of μ, more precisely $|\mu| > M$, the $\tilde{e}_R$ decays to 100 % into $\tilde{\chi}_1^0$. This can be understood because the $\tilde{e}_R$ couples only to the B-ino component of the neutralinos, and $\tilde{\chi}_1^0$ is essentially a B-ino in this parameter region. For $|\mu| < M$, the decays into $\tilde{\chi}_2^0$ and $\tilde{\chi}_3^0$ are significant because here these particles have large B-ino components.

Concerning the $\tilde{e}_L$ decays, the direct decay into $\tilde{\chi}_1^0$ is not the most important one. For $|\mu| \gtrsim M$ the decay into the light chargino dominates, the branching ratio being between 40 % and 50 % . For $|\mu| \lesssim M$ the decays into $\tilde{\chi}_2^0$ and $\tilde{\chi}_3^0$ can have large branching ratios because in this region the heavy neutralinos have large gaugino components.

Despite the possibility of cascade decays the most interesting signature for pair production of $\tilde{e}_R$ or $\tilde{e}_L$ is again provided by the two-sided events with acollinear, acoplanar, hard electrons plus missing energy. The rate for $e^+e^- \to \tilde{e}_R^+\tilde{e}_R^- \to e^+ + e^- + \not{p}$ can go up to 180 fb for $m_{\tilde{e}_R} = 200$ GeV and $\tan\beta = 4$, whereas the corresponding one for $e^+e^- \to \tilde{e}_L^+\tilde{e}_L^- \to e^+ + e^- + \not{p}$ reaches 60 fb.

A Monte Carlo study of selectron production is given in [22].

3.2.4 Sneutrino production

The cross section for $e^+e^- \to \tilde{\nu}_e + \bar{\tilde{\nu}}_e$ is in general higher than that for selectron production because the Z^0 and the charginos couple more strongly. For $m_{\tilde{\nu}_e} = 200$ GeV the cross section can reach 700 fb.

The sneutrino can only be observed if it decays first into a chargino or a higher mass neutralino (see eq. (3.12), which then decays into leptons or quarks. Only if $M < m_{\tilde{\nu}_e}$ or $|\mu| < m_{\tilde{\nu}_e}$, the sneutrino is visible. It turns out that in this region the decay into the light chargino has the largest branching ratio. Therefore, the important signatures are again one-sided and two-sided events with hard leptons and jets, as already discussed for LEP200 (see Sect. 3.1.4). More details on pair production of sneutrinos as well as of the other sfermions ($\tilde{\mu}_{L,R}, \tilde{\nu}_\mu, \tilde{u}_{L,R}, \tilde{d}_{L,R}$ etc.) can be found in [19]. A Monte Carlo study of smuon production is given in [23].

4 pp Collisions

In pp collisions one expects the strongly interacting SUSY particles, gluinos and squarks, to be produced with the largest cross section of all supersymmetric particles [24, 25].

The basic processes for gluino and squark production in hadronic collisions are [26]

$$\begin{aligned} g+g &\rightarrow \tilde{g}+\tilde{g} & (4.1)\\ q+\bar{q} &\rightarrow \tilde{g}+\tilde{g} & (4.2)\\ g+g &\rightarrow \tilde{q}+\bar{\tilde{q}} & (4.3)\\ q+\overset{(-)}{q} &\rightarrow \tilde{q}+\overset{(-)}{\tilde{q}} & (4.4)\\ g+\overset{(-)}{q} &\rightarrow \tilde{g}+\overset{(-)}{\tilde{q}}\,. & (4.5) \end{aligned}$$

For example, for a gluino mass $m_{\tilde{g}} = 500$ GeV one obtains at $\sqrt{s} = 16$ TeV, the design c.m. energy of the LHC, a production cross section of ~ 50 pb for $pp \rightarrow \tilde{g}\tilde{g}+X$. Similarly, for a squark mass $M_{\tilde{q}} = 500$ GeV one gets a cross section of ~ 15 pb for $pp \rightarrow \tilde{q}\bar{\tilde{q}}+X$. Assuming an integrated luminosity of 10^5 pb^{-1} this would mean a rate of 5×10^6 gluino pairs and 1.5×10^6 squark pairs per year. For the SSC one obtains a cross section $\sigma \approx 10$ pb for $pp \rightarrow \tilde{g}\tilde{g}+X$ at $\sqrt{s} = 40$ TeV and $m_{\tilde{g}} = 1000$ GeV. Taking an integrated luminosity of 10^4 pb^{-1} yields 10^5 such events per year.

If squarks are heavier than gluinos then the gluinos produced decay into

$$\begin{aligned} \tilde{g} &\rightarrow q+\bar{q}+\tilde{\chi}_i^0 & (4.6)\\ &\rightarrow t+\bar{t}+\tilde{\chi}_i^0 & (4.7)\\ &\rightarrow q+\bar{q}'+\tilde{\chi}_i^{\pm}, & (4.8)\\ &\rightarrow t+\bar{b}+\tilde{\chi}_i^-,\ \bar{t}+b+\tilde{\chi}_i^+ & (4.9)\\ &\rightarrow g+\tilde{\chi}_i^0. & (4.10) \end{aligned}$$

Here we distinguish between decays into light quarks q and those which involve the top quark because they show a different decay pattern. This is due to the fact that in the decays (4.7) and (4.9) the top Yukawa coupling and additional quark mass terms are important. The decays (4.6 - 4.9) proceed via virtual squark exchange. The decay into a gluon, eq. (4.10), is possible via quark-squark loops, the $t-\tilde{t}$ contribution being the most important one. It is not negligible in certain regions of the SUSY parameter space.

In the mass range for gluinos and squarks we shall consider, also the charginos and neutralinos will be heavy. Therefore, in most cases they will decay into $W^{\pm}, Z^0$ or Higgs particles and lower mass states of charginos or neutralinos according to eqs. (3.9) and (3.10). If these two-body decays are kinematically not allowed, the three-body decays, eqs. (3.7) and (3.8), may also become important. Thus in general one has cascade decays of gluinos. They end when the lightest supersymmetric particle $\tilde{\chi}_1^0$ is reached. The final states can therefore contain Z^0-bosons, $W^{\pm}$-bosons, neutral and charged Higgs-bosons, leptons and jets and missing momentum from the lightest neutralino and the neutrinos.

If the gluinos are heavier than the squarks, then squark production will be more important. In the case of light quark flavours the squarks then decay according to eq. (3.13). For the following decays of the top squark and the bottom squark

$$\begin{aligned} \tilde{t}_{L,R} &\rightarrow t+\tilde{\chi}_i^0 & (4.11)\\ \tilde{t}_R &\rightarrow b+\tilde{\chi}_i^+ & (4.12)\\ \tilde{b}_L &\rightarrow t+\tilde{\chi}_i^- & (4.13) \end{aligned}$$

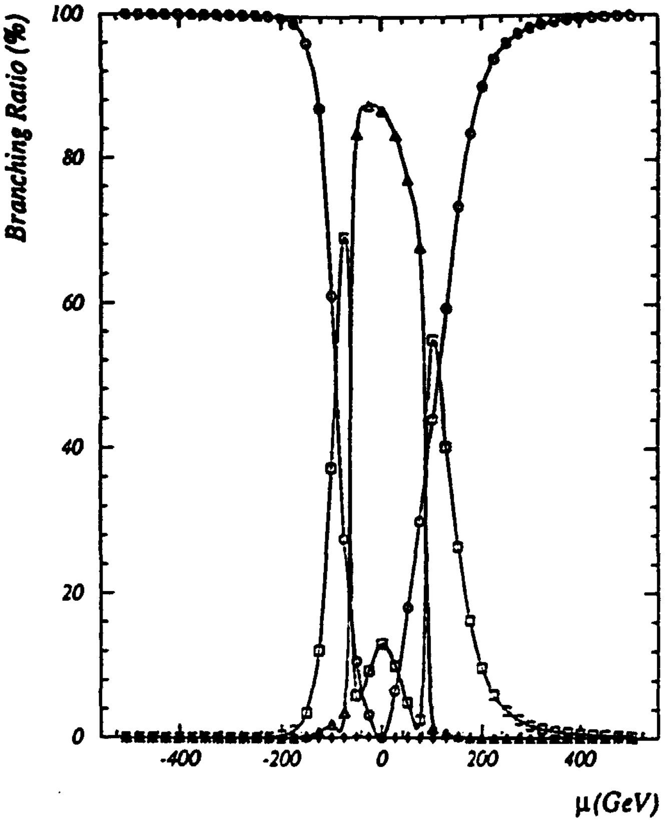

Fig. 11a: Branching ratios for $\tilde{e}_R^- \to e^- \tilde{\chi}_i^0$, as a function of μ, for $m_{\tilde{e}_{L,R}} = 200$ GeV, $M = 150$ GeV, $\tan\beta = 4$, $\sin^2\theta_W = 0.23$. The curves correspond to the following transitions:

- o into $\tilde{\chi}_1^0$
- □ into $\tilde{\chi}_2^0$
- △ into $\tilde{\chi}_3^0$
- ◇ into $\tilde{\chi}_4^0$

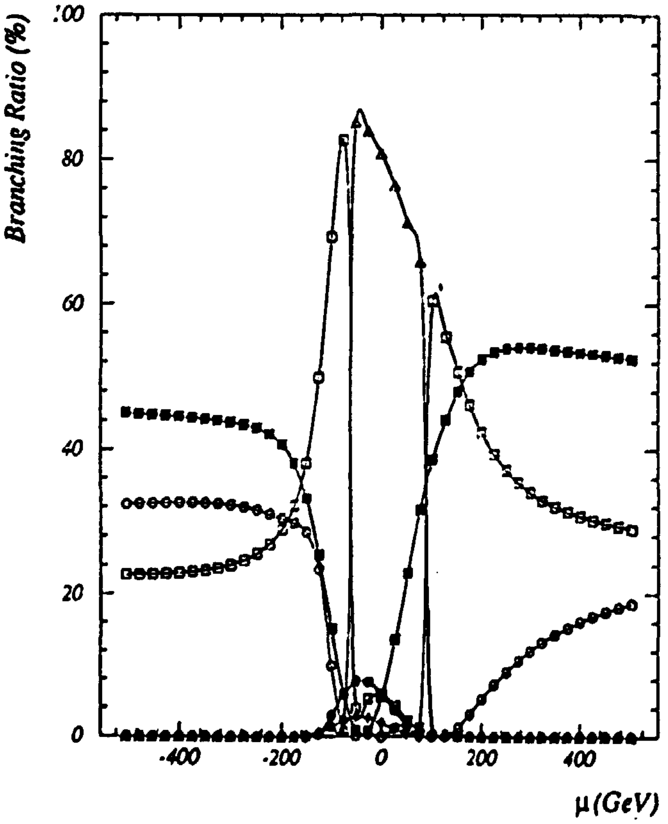

Fig. 11b: Branching ratios for $\tilde{e}_L^- \to e^- \tilde{\chi}_i^0, \nu \tilde{\chi}_i^-$, as a function of μ, for $m_{\tilde{e}_{L,R}} = 200$ GeV, $M = 150$ GeV, $\tan\beta = 4$, $\sin^2\theta_W = 0.23$. The curves correspond to the following transitions:

- ▪ into the light chargino $\tilde{\chi}_1^\pm$
- • into the heavy chargino $\tilde{\chi}_2^\pm$
- o into $\tilde{\chi}_1^0$
- □ into $\tilde{\chi}_2^0$
- △ into $\tilde{\chi}_3^0$
- ◇ into $\tilde{\chi}_4^0$.

it is again necessary to take into account the top Yukawa coupling. (Notice that the Yukawa coupling terms in $\tilde{t}_L \to b + \tilde{\chi}_i^+$ and $\tilde{b}_R \to t + \tilde{\chi}_i^-$ are proportional to the bottom quark mass which we shall neglect here.)

The neutralinos and charginos again decay as described above. Also here a variety of cascade decays is possible until the lightest neutralino is produced.

For illustration we show in Fig. 12 the domains in the (M, μ) plane (for $\tan\beta = 4$) where for a squark with a mass of 500 GeV cascade decays are kinematically possible (domain I), or where only transitions into the lightest neutralino are allowed (domain II). For a gluino with a mass of 500 GeV the same picture as in Fig. 12 is valid taking $M \simeq 0.3\, m_{\tilde{g}}$.

In pp collisions sleptons, charginos and neutralinos could also be produced by the Drell-Yan mechanism, but their cross sections are smaller [27] and are not considered here.

4.1 Gluino decays and signatures

In order to understand the complex decay pattern of gluinos and squarks it is necessary to consider the individual steps in the cascade. For the decays we have used the formulae as given in [28] where a complete list of these is presented.

Considering first only the gluino decays into light quarks, $\tilde{g} \to q + \bar{q} + \tilde{\chi}_i^{0,\pm}$, and leaving out the decay $\tilde{g} \to g + \tilde{\chi}_i^0$, the overall picture of gluino decays would be rather simple [29] because then only the gaugino components of the neutralinos couple: For $|\mu| \lesssim m_{\tilde{g}}/3$ mainly the heavy chargino and the heaviest neutralino are produced, the light chargino and the two lightest neutralinos being mainly higgsinos. For $|\mu| \gtrsim m_{\tilde{g}}/3$ the decays into the light chargino and the second lightest neutralino would dominate, because here the heavy particles are higgsino like. This is illustrated in Fig. 13 for $m_{\tilde{g}} = 750$ GeV and $\tan\beta = 4$. (Furthermore, we have taken $M_{\tilde{q}_L} = M_{\tilde{q}_R} = 2m_{\tilde{g}}$, $\alpha_s = 0.1$, and $\sin^2\theta_W = 0.23$.)

This simple picture is changed if in the decays $\tilde{g} \to t + \bar{t} + \tilde{\chi}_i^0$, $\tilde{g} \to t + \bar{b} + \tilde{\chi}_i^-$, $\tilde{g} \to b + \bar{t} + \tilde{\chi}_i^+$ the top mass is taken into account [28, 30]. (We take $m_t = 150$ GeV.) In the parameter domain $|\mu| \lesssim m_{\tilde{g}}/3$ the dominant transition of these decays is now that into the light chargino, contrary to the simple picture described above. For $|\mu| > m_{\tilde{g}}/3$ the influence of the Yukawa coupling terms is smaller because the higgsino-like particles are now heavy and, therefore, reduce the phase space, a feature which is even more pronounced for smaller gluino masses.

The decays $\tilde{g} \to g + \tilde{\chi}_i^0$ play a minor rôle. In the cases considered the sum of the branching ratios for $\tilde{g} \to g + \tilde{\chi}_i^0$ is a few percent. It can, however, be larger for smaller gluino masses and smaller $\tan\beta$ [28, 30].

The branching ratios for $\tilde{g} \to \tilde{\chi}_i^0 + q + \bar{q}$ (or g) and $\tilde{g} \to \tilde{\chi}_i^\pm + q + \bar{q}'$, summed over all quark flavours including the top quark, are shown in Fig. 14 as a function of μ for $m_{\tilde{g}} = 750$ GeV, $\tan\beta = 4$. For $|\mu| \lesssim m_{\tilde{g}}/3$ there are substantial transition rates into the light chargino and the light neutralinos. For $|\mu| > m_{\tilde{g}}/3$ the transitions into the light chargino and the second lightest neutralino are the most important ones. Notice that the branching ratio for the decay into the lightest neutralino is only about 15 percent. It is smaller than that of the decay into $\tilde{\chi}_2^0$ because for larger $|\mu|$ the $\tilde{\chi}_1^0$ is mainly a B-ino and the $\tilde{\chi}_2^0$ a W^3-ino. Notice that the decay into $\tilde{\chi}_3^0$ appears due to $\tilde{g} \to g + \tilde{\chi}_3^0$ and $\tilde{g} \to t + \bar{t} + \tilde{\chi}_3^0$.

Next we discuss some interesting signatures for gluino production $p + p \to \tilde{g} + \tilde{g} + X$ (assuming that the squarks are heavier than gluinos). The 'classical' signature would be that both gluinos go directly into the lightest supersymmetric particle $\tilde{\chi}_1^0$, leading to events

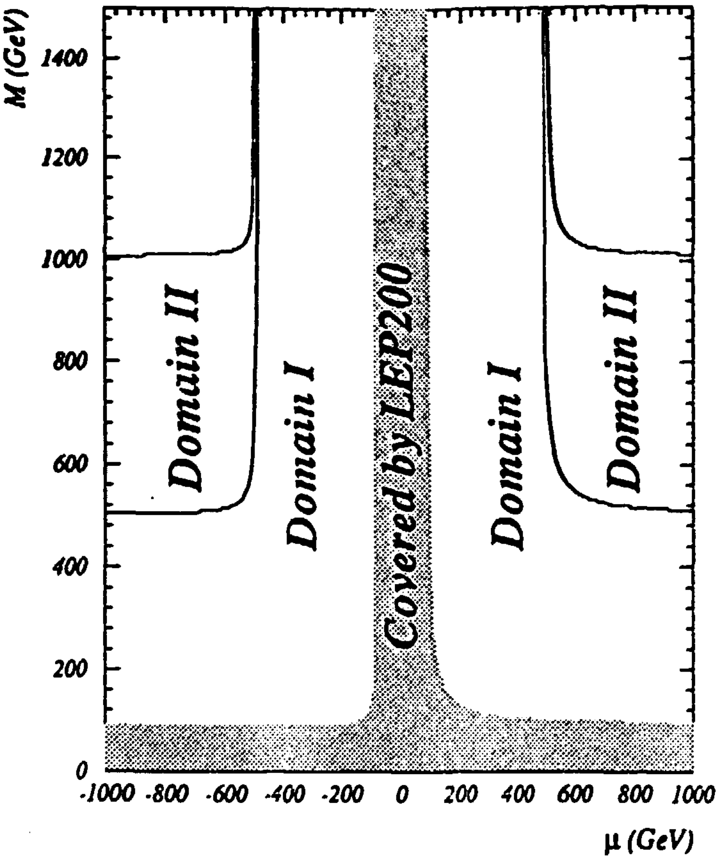

Fig. 12: Supersymmetry parameter space (M, μ) for decays of a squark with $M_{\tilde{q}} = 500$ GeV, $\tan\beta = 4$. Domain I: Cascade decays possible. Domain II: Only transitions into $\tilde{\chi}_1^0$ possible. Also shown the region covered by LEP200. For a gluino with $m_{\tilde{g}} = 500$ GeV the same figure is valid taking $M \simeq 0.3\, m_{\tilde{g}}$. For another squark mass an analogous figure holds if M and μ are scaled by the ratio of the squark masses.

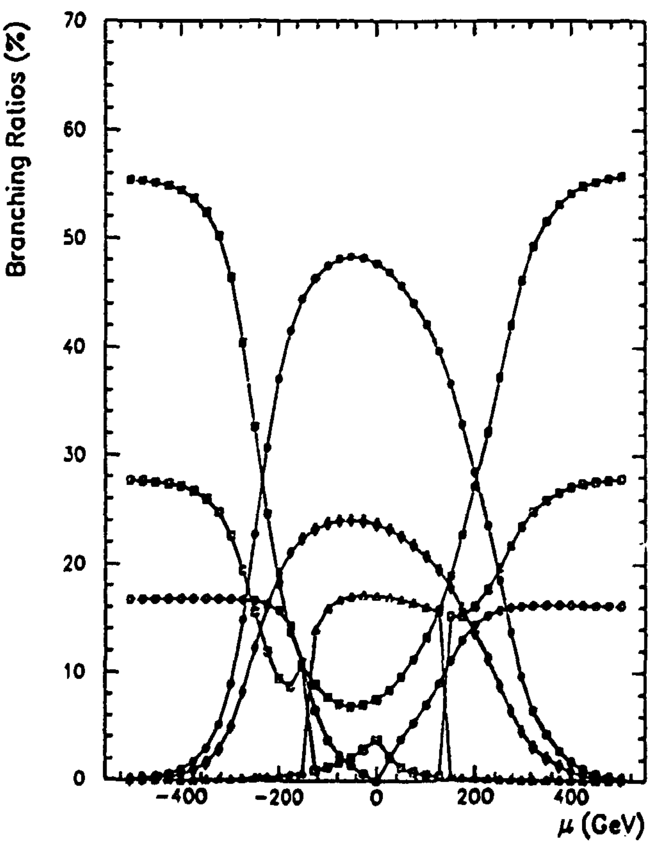

Fig. 13: Branching ratios for the decays $\tilde{g} \to q + \bar{q} + \tilde{\chi}_i^0$, $\tilde{g} \to u + \bar{d} + \tilde{\chi}_i^-$ plus $d + \bar{u} + \tilde{\chi}_i^+$, neglecting all quark masses, as a function of μ for $m_{\tilde{g}} = 750$ GeV and $\tan\beta = 4$. Here the decays $\tilde{g} \to g + \tilde{\chi}_i^0$ are left out. We have taken $M_{\tilde{q}_L} = M_{\tilde{q}_R} = 2m_{\tilde{g}}$, $\alpha_s = 0.1$, and $\sin^2\theta_W = 0.23$. The curves correspond to the following transitions:

- ▪ into the light chargino $\tilde{\chi}_1^\pm$
- • into the heavy chargino $\tilde{\chi}_2^\pm$
- ∘ into $\tilde{\chi}_1^0$
- □ into $\tilde{\chi}_2^0$
- △ into $\tilde{\chi}_3^0$
- ◇ into $\tilde{\chi}_4^0$.

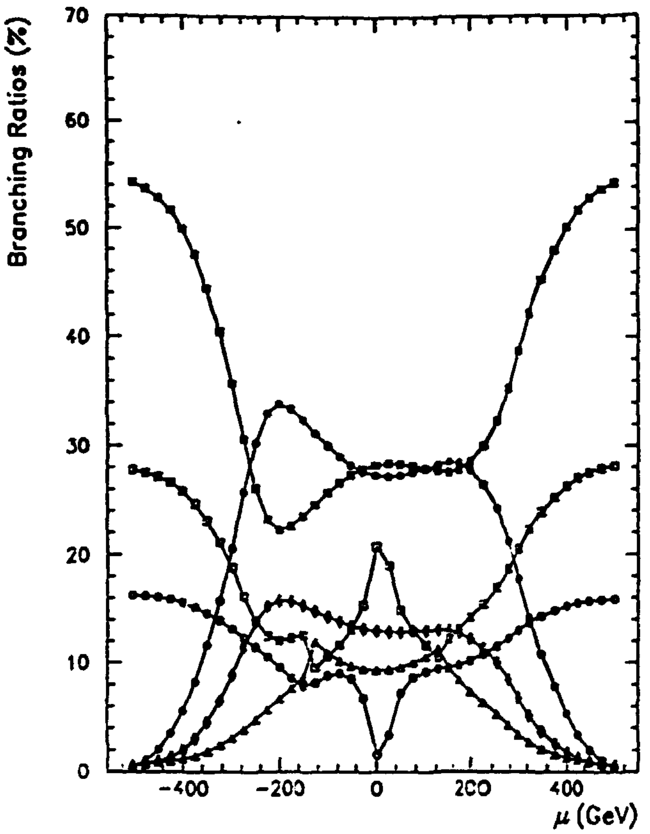

Fig. 14: Branching ratios for $\tilde{g} \to \tilde{\chi}_i^0 + q + \bar{q}$, $\tilde{\chi}_i^0 + g$ and $\tilde{g} \to \tilde{\chi}_j^+ + q + \bar{q}'$ plus $\tilde{\chi}_j^- + \bar{q} + q'$, summed over all quark flavours, as a function of μ, for $m_{\tilde{g}} = 750$ GeV and $\tan\beta = 4$. We have taken $m_t = 150$ GeV, $M_{\tilde{q}_L} = M_{\tilde{q}_R} = 2m_{\tilde{g}}$, $\alpha_s = 0.1$, and $\sin^2\theta_W = 0.23$. The curves correspond to the following transitions:

- ■ into the light chargino $\tilde{\chi}_1^\pm$
- ● into the heavy chargino $\tilde{\chi}_2^\pm$
- ○ into $\tilde{\chi}_1^0$
- □ into $\tilde{\chi}_2^0$
- △ into $\tilde{\chi}_3^0$
- ◇ into $\tilde{\chi}_4^0$.

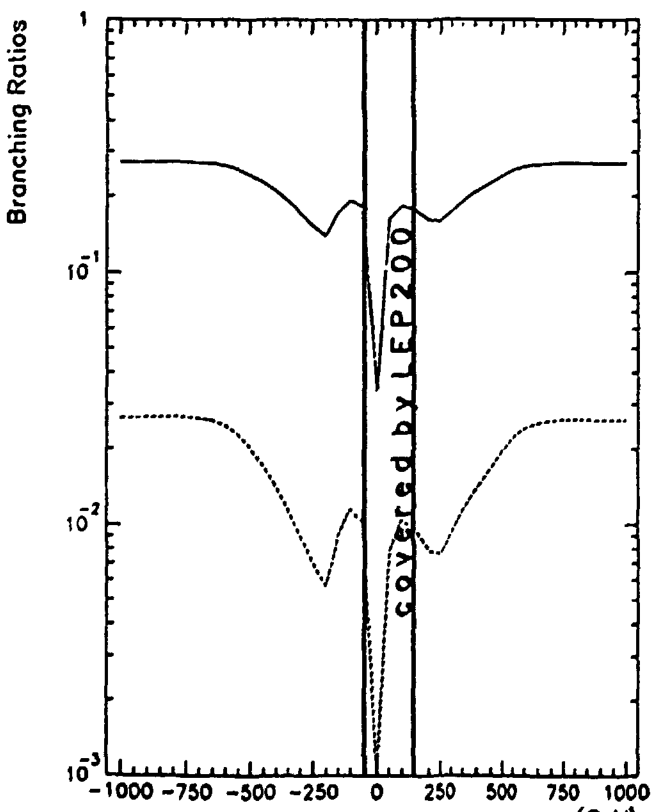

Fig. 15: The branching ratios for the two produced gluinos to go directly into $\tilde{\chi}_1^0$ and $2\,\tilde{\chi}_1^0$; i.e. $\tilde{g} + \tilde{g} \to \tilde{\chi}_1^0 + X$ (——), and $\tilde{g} + \tilde{g} \to \tilde{\chi}_1^0 + \tilde{\chi}_1^0 + X$ (- - -), (where X does not contain another $\tilde{\chi}_1^0$) for $m_{\tilde{g}} = 1000$ GeV as a function of μ, for $\tan\beta = 4$. We have taken $m_t = 150$ GeV, $M_{\tilde{q}_L} = M_{\tilde{q}_R} = 2m_{\tilde{g}}$, $\alpha_s = 0.1$, and $\sin^2\theta_W = 0.23$. Also shown the region covered by LEP200.

with large missing energy. This is shown in Fig. 15 for $m_{\tilde{g}} = 1000$ GeV. The branching ratio for both gluinos going directly into the LSP is at most a few percent. Thus with an integrated luminosity of 10^5 pb^{-1} one could expect $\sim 10^3$ such events at the LHC. Similarly at the SSC one would have 2×10^3 such events. The probability that only one gluino decays directly into $\tilde{\chi}_1^0$ is higher and can go up to 30 percent, as also shown in Fig. 15. The region in μ which will be explored by LEP 200 is also indicated.

A further interesting signature would be two Z^0's in the final state which originate from the cascade decays. Fig. 16 shows the branching ratio for $\tilde{g} + \tilde{g} \to 2\,Z^0 + X$ for a gluino mass of 1000 GeV. (We have taken the mass of the Higgs particle h^0, $m_{h^0} = 80$ GeV, and the masses of all other Higgs particles much heavier.) The branching ratio can go up to 10 %, but there is a strong dependence on the SUSY parameter μ.

Fig. 16 also shows the branching ratios for $\tilde{g} + \tilde{g} \to 4\,\mu$'s, $5\,\mu$'s, and $6\,\mu$'s. Here it is summed over all events with muons coming from Z^0, $W^\pm$, t-quark decays into bW, and three-body decays of charginos and neutralinos. Over a large range of μ the four muon rate is about 10^{-4}.

We want to emphasize that some details of the $2\,Z^0$ and multimuon rates depend on the mass spectrum in the Higgs sector. If the decay of a chargino or a neutralino into a Higgs particle is possible the other decay rates are reduced.

A more detailed discussion of gluino signatures is given in [31]. Monte Carlo studies taking into account the standard model background ($t\bar{t}$, Z^0Z^0 production, etc.) were performed and have shown that at the LHC gluinos in the mass range 300 GeV $\leq m_{\tilde{g}} \leq$ 1000 GeV can be detected [25, 27].

4.2 Squark decays and signatures

As to the squark decays, one has again to distinguish between those into light quarks and heavy quarks, and of course between left and right squarks. All cases were discussed in detail in [28] where also the corresponding formulae are given.

If the quark masses can be neglected the pattern of squark decays according to eq. (3.13) is again rather simple. The branching ratios for right squarks are then the same (independent of flavour) as for right selectrons of the same mass. These are already shown in Fig. 11a. For $|\mu| > M$ right squarks decay practically 100 % into $\tilde{\chi}_1^0$, and for $|\mu| < M$ to more than 90 % into $\tilde{\chi}_3^0$.

Left squarks decay dominantly into charginos as can be seen in Fig. 17 where we plot the branching ratios of $\tilde{u}_L \to d + \tilde{\chi}_i^+$, $u + \tilde{\chi}_i^0$, for $M_{\tilde{q}} = 1000$ GeV. For $|\mu| > M$ ($|\mu| < M$) the transition into the lighter (heavier) chargino has the largest branching ratio due to its gaugino nature in this region of μ. Among the decays into neutralinos, for $|\mu| > M$ ($|\mu| < M$) the transitions into $\tilde{\chi}_2^0$ ($\tilde{\chi}_4^0$) have also big rates as the $\tilde{\chi}_2^0$ ($\tilde{\chi}_4^0$) is mainly a W^3-ino in this region of μ. A qualitatively similar pattern holds for $\tilde{d}_L$ decays.

The influence of the top quark mass terms in the decays of $\tilde{t}_R$ is seen in Fig. 18 where we plot the branching ratios into charginos and neutralinos as a function of μ for $M_{\tilde{q}} = 1000$ GeV, $M = 500$ GeV, $\tan\beta = 4$. Now the decays into charginos become very important, for $|\mu| \lesssim M$ the decay into $\tilde{\chi}_1^+$ being the dominant one. In the $\tilde{t}_L$ decays the top Yukawa coupling only changes the width of $\tilde{t}_L \to t + \tilde{\chi}_i^0$.

As to the $\tilde{b}_L$ decays, the main differences between these and the decays of $\tilde{d}_L$ appear again in the region $|\mu| \lesssim M$. Due to the top Yukawa coupling the width for $\tilde{b}_L \to t + \tilde{\chi}_1^-$ becomes the largest one.

Concerning the signatures for squark production $p + p \to \tilde{q} + \bar{\tilde{q}} + X$, one expects the direct transition of a squark into the lightest supersymmetric particle $\tilde{\chi}_1^0$ to be more

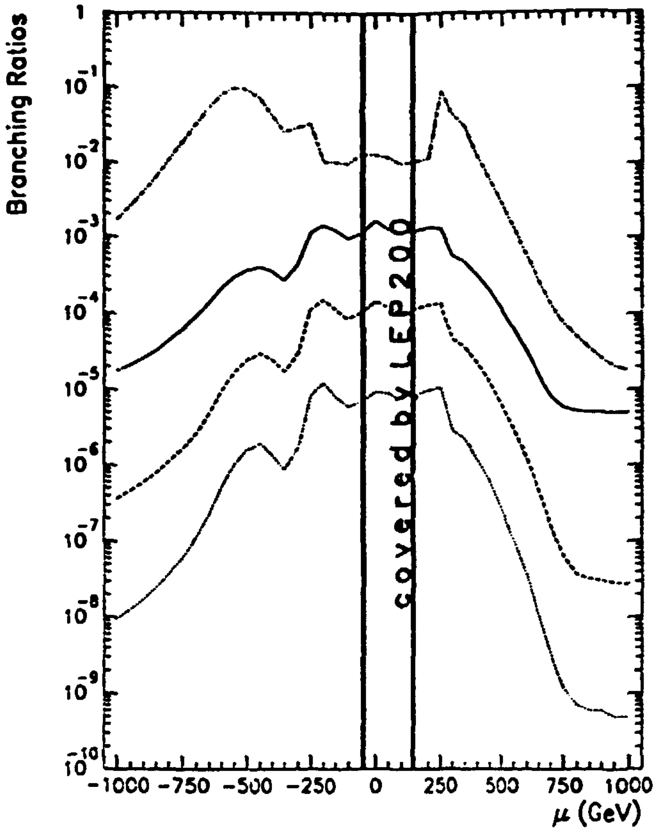

Fig. 16: The branching ratios for $\tilde{g}+\tilde{g} \rightarrow 2Z^0 + X$ (- · - · -), $\tilde{g}+\tilde{g} \rightarrow 4\mu + X$ (——), $\tilde{g}+\tilde{g} \rightarrow 5\mu + X$ (- - -), $\tilde{g}+\tilde{g} \rightarrow 6\mu + X$ (· · · ·) for $m_{\tilde{g}} = 1000$ GeV, as a function of the parameter μ, for $\tan\beta = 4$. We have summed over all events with muons coming from Z^0, $W^{\pm}$, and three body decays of charginos and neutralinos, and from $t \rightarrow Wb$. We have taken $m_t = 150$ GeV, $M_{\tilde{q}_L} = M_{\tilde{q}_R} = 2m_{\tilde{g}}$, $\alpha_s = 0.1$, $\sin^2\theta_W = 0.23$, $m_{A^0} = 80$ GeV and all other Higgs particles heavy. Also shown the region covered by LEP200.

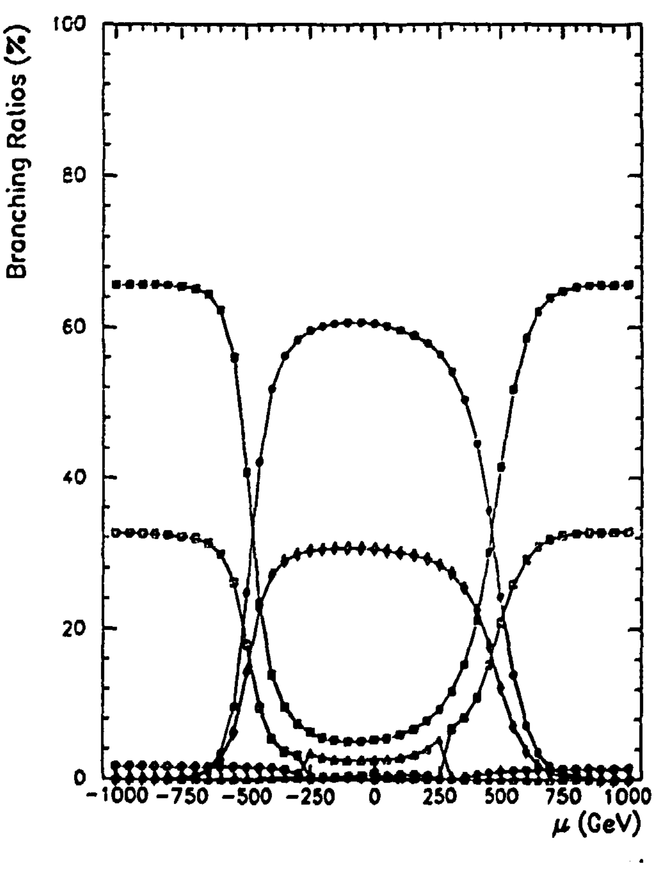

Fig. 17: Branching ratios for $\tilde{u}_L$ decays into charginos and neutralinos for $u_L \rightarrow d + \tilde{\chi}_i^+$, $u + \tilde{\chi}_i^0$, as a function of μ, for $M_{\tilde{q}} = 1000$ GeV, $M = 500$ GeV, $\tan\beta = 4$. We have taken $m_t = 150$ GeV, $\alpha_s = 0.1$, $\sin^2\theta_W = 0.23$. The curves correspond to the following transitions:

- ■ into the light chargino $\tilde{\chi}_1^{\pm}$
- ● into the heavy chargino $\tilde{\chi}_2^{\pm}$
- ○ into $\tilde{\chi}_1^0$
- □ into $\tilde{\chi}_2^0$
- △ into $\tilde{\chi}_3^0$
- ◇ into $\tilde{\chi}_4^0$.

important than for gluinos because right squarks of light flavours decay into $\tilde{\chi}_1^0$ to more than 90 percent (for $|\mu| \gtrsim M$). Fig. 19 exhibits the branching ratios for $\tilde{q}+\bar{\tilde{q}} \to \tilde{\chi}_1^0 + X$ and $\tilde{q}+\bar{\tilde{q}} \to \tilde{\chi}_1^0 + \tilde{\chi}_1^0 + X$, i.e. only one of the squarks or both directly decay into $\tilde{\chi}_1^0$, for $M_{\tilde{q}} = 1000$ GeV, $\tan\beta = 4$, and $M = 500$ GeV. We have averaged over left and right squarks and all flavours. It is interesting to note that in a large range of μ the branching ratio into two $\tilde{\chi}_1^0$ is an order of magnitude larger than that into one $\tilde{\chi}_1^0$. As a consequence, about 40 % of the events where a $\tilde{q}\bar{\tilde{q}}$ pair is produced will have the 'classical' signature of large missing energy. This feature is quite independent of $\tan\beta$ and holds in a large range of squark masses, provided $|\mu| \gtrsim M$.

Other signatures would be $\tilde{q}+\bar{\tilde{q}} \to ZZ+X, 4\mu+X, 5\mu+X$, etc. They are discussed in [31]. Monte Carlo studies [25, 27] have shown that also for squarks a mass reach of about 1 TeV is possible at LHC.

5 ep Collisions

The processes most favourable for finding supersymmetric particles in ep collisions are the reactions [32, 33, 34]

$$e+p \;\to\; \tilde{e}_{L,R} + \tilde{q}_{L,R} + X \tag{5.1}$$
$$e+p \;\to\; \tilde{\nu}_L + \tilde{q}_L + X, \tag{5.2}$$

The basic reaction mechanism is $eq \to \tilde{e}_{L,R}\,\tilde{q}_{L,R}$ or $eq \to \tilde{\nu}\tilde{q}_L$ scattering via t channel neutralino or chargino exchange. The sea quarks and the antiquarks in the proton also contribute, though their contribution is smaller.

The produced slepton or squark decays into the corresponding fermion and a neutralino $\tilde{\chi}_i^0$ or chargino $\tilde{\chi}_i^\pm$, eqs. (3.11 – 3.13). (Here we assume that the gluino is heavier than the squarks.) The higher mass neutralinos and charginos then further decay until the LSP is reached, see eqs. (3.7 – 3.10). Therefore, also here cascade decays are possible.

The production cross sections for both reactions (5.1 – 5.2) depend most strongly on the sum of the masses of the slepton and squark produced, and of course on the centre of mass energy.

5.1 HERA

At HERA ep collisions at $\sqrt{s} = 314$ GeV will be studied. The design luminosity is 1.5×10^{31} cm^{-2}s^{-1}. The reactions (5.1 – 5.2) have been studied for this energy in [33, 34]. Cross sections larger than 0.1 pb have been found for $m_{\tilde{e},\tilde{\nu}}+m_{\tilde{q}} \lesssim 180$ GeV. If cross sections down to 5×10^{-2} pb can be measured, the observable mass range extends to $m_{\tilde{e},\tilde{\nu}}+m_{\tilde{q}} \lesssim 200$ GeV. With the exisiting experimental bounds on the squark and selectron masses from CDF and LEP (see Sect. 2) and within the MSSM, the possibilities of detecting SUSY particles at HERA are therefore limited. At a higher c.m. energy, e.g. $\sqrt{s} = 450$ GeV, the mass range $m_{\tilde{e},\tilde{\nu}} + m_{\tilde{q}} \leq 300$ GeV could be explored.

Relaxing the MSSM by including R-parity violating terms would allow single SUSY particle production and thus extend the explorable mass region for SUSY particles. For further studies we refer to [35].

5.2 LEP/LHC

The LHC will offer the unique possibility of being operated also in the ep collider mode at $\sqrt{s} = 1.4$ TeV with a luminosity of about 10^{32} cm^{-2}s^{-1}. Also here the search for SUSY particles will be an interesting subject. Such an ep collider will substantially extend the explorable mass region, especially for selectrons and sneutrinos [36, 37].

In Fig. 20 we show the cross section for $e^- p \to \tilde{e}_{L,R} + \tilde{q}_{L,R} + X$ as a function of the sfermion mass, summed over all possible pairs of selectrons and squarks, taking $m_{\tilde{e}} = m_{\tilde{q}}$, for $\mu = -200$ GeV and various values of M. These cross sections are larger than 0.1 pb for $m_{\tilde{f}} \lesssim 300$ GeV. More generally, the cross section is larger than 0.1 pb for $m_{\tilde{e}} + m_{\tilde{q}} \leq$ 600 GeV. Therefore, sfermions in this mass range would give between 50 and 1000 events per year (assuming an integrated luminosity of 500 pb^{-1}). The production cross section for sneutrinos is in general larger than that for selectrons because the chargino couplings are stronger than the neutralino couplings.

In Fig. 20 also the dependence on the SUSY paramter M can be seen. The cross section varies approximately within a factor of 2 for $m_{\tilde{e}} = m_{\tilde{q}} = 250$ GeV and in the parameter range 200 GeV $\leq M \leq 800$ GeV. The dependence on μ and $\tan\beta$ is rather weak.

The individual production cross sections for different slepton and squark species are very different from each other. $\sigma(e^- p \to \tilde{\nu}_L + \bar{\tilde{d}}_L + X)$ is in general the largest cross section due to the larger couplings of charginos to sleptons and squarks. In selectron production $ep \to \tilde{e}_L + \tilde{u}_L + X$ has the largest cross section.

To find suitable signatures of SUSY particle production in ep collisions a proper treatment of all the decays is necessary. Selectron, sneutrino and squark decays have already been discussed in detail in Sect. 3.2 and 4.2.

The signatures substantially depend on the supersymmetry parameters M and μ, or more precisely, whether cascade decays are possible or not. A good signature for selectron production is one isolated electron + missing energy on the lepton side. For $m_{\tilde{f}} = 250$ GeV we get a rate of ~ 0.1 pb. A signature for sneutrino production is a lepton pair e^+e^- (or μ^+e^-) + missing energy on the lepton side. If cascade decays of the sneutrino are possible the cross section for such events is ~ 0.01 pb. More details can be found in [38].

Monte Carlo studies taking into account the background have shown that detection of selectron and squark production in the mass range $m_{\tilde{e}} + m_{\tilde{q}} \leq 600$ GeV should be possible [39].

6 Summary

Here we have presented a systematic and rather complete study of supersymmetric particle production and decay within the Minimal Supersymmetric Standard Model in e^+e^-, pp, and ep collisions at high energies. The prospects of searching for supersymmetry in experiments to be performed at HERA, LEP200, LHC, SSC, LEP/LHC and at a 500 GeV e^+e^- collider are investigated in the corresponding supersymmetry parameter domain. Production and in particular the decays of supersymmetric particles depend in a characteristic way on the supersymmetry parameters. A general feature is that cascade decays become more important with increasing particle mass, leading to a complex decay pattern. Furthermore, this strongly influences the signatures for supersymmtry. Quite generally, the "classical" signature, large missing momentum, will be weakened. Instead of it, new signatures as $W^\pm, Z^0$, Higgs particles in the final state will appear.

Within the next years, experiments at FNAL will extend the mass range for gluinos and squarks beyond 200 GeV. At HERA sleptons and squarks are detectable if approximately $m_{\tilde{e},\tilde{\nu}} + m_{\tilde{q}} \leq 180$ GeV. Non-strongly interacting supersymmetric particles, in particular sleptons and charginos, will be observed at LEP200 if their mass is below 90 GeV.

A big step forward in the search for supersymmetry is possible by the pp colliders LHC and SSC. A mass range for gluinos and squarks up to the TeV region will be explored.

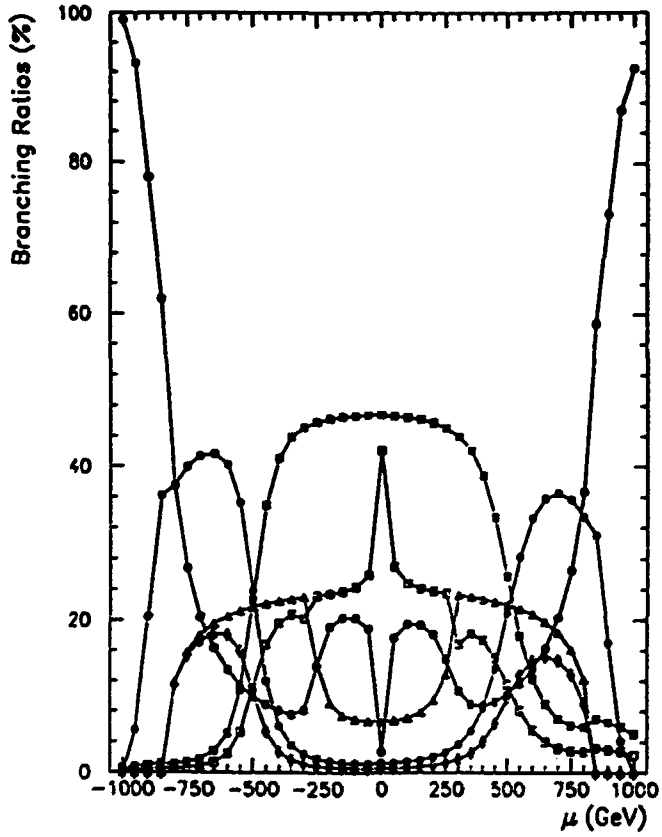

Fig. 18: Branching ratios for $\tilde{t}_R$ decays into charginos and neutralinos for $\tilde{t}_R \to b + \tilde{\chi}_i^+, t + \tilde{\chi}_i^0$, as a function of μ, for $M_{\tilde{q}} = 1000$ GeV, $M = 500$ GeV, $\tan\beta = 4$. We have taken $m_t = 150$ GeV, $\alpha_s = 0.1$, $\sin^2\theta_W = 0.23$. The curves correspond to the following transitions:
- ▪ into the light chargino $\tilde{\chi}_1^\pm$
- • into the heavy chargino $\tilde{\chi}_2^\pm$
- ∘ into $\tilde{\chi}_1^0$
- □ into $\tilde{\chi}_2^0$
- △ into $\tilde{\chi}_3^0$
- ◇ into $\tilde{\chi}_4^0$.

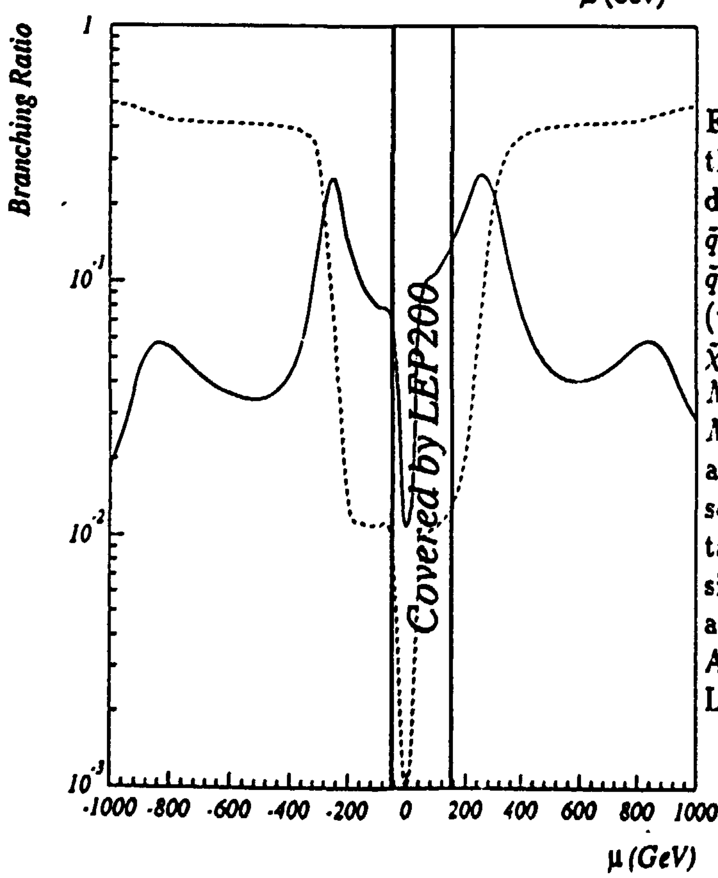

Fig. 19: The branching ratios for the two produced squarks to go directly into $\tilde{\chi}_1^0$ and $2\tilde{\chi}_1^0$, i.e. $\tilde{q} + \bar{\tilde{q}} \to \tilde{\chi}_1^0 + X$ (——) and $\tilde{q} + \bar{\tilde{q}} \to \tilde{\chi}_1^0 + \tilde{\chi}_1^0 + X$ (- - -), (where X does not contain another $\tilde{\chi}_1^0$) as a function of μ for $M_{\tilde{q}_L} = M_{\tilde{q}_R} = 1000$ GeV, $M = 500$ GeV, $\tan\beta = 4$. We have averaged over left and right squarks and all flavours. We have taken $m_t = 150$ GeV, $\alpha_s = 0.1$, $\sin^2\theta_W = 0.23$, $m_{h^0} = 80$ GeV and all other Higgs particles heavy. Also shown the region covered by LEP200.

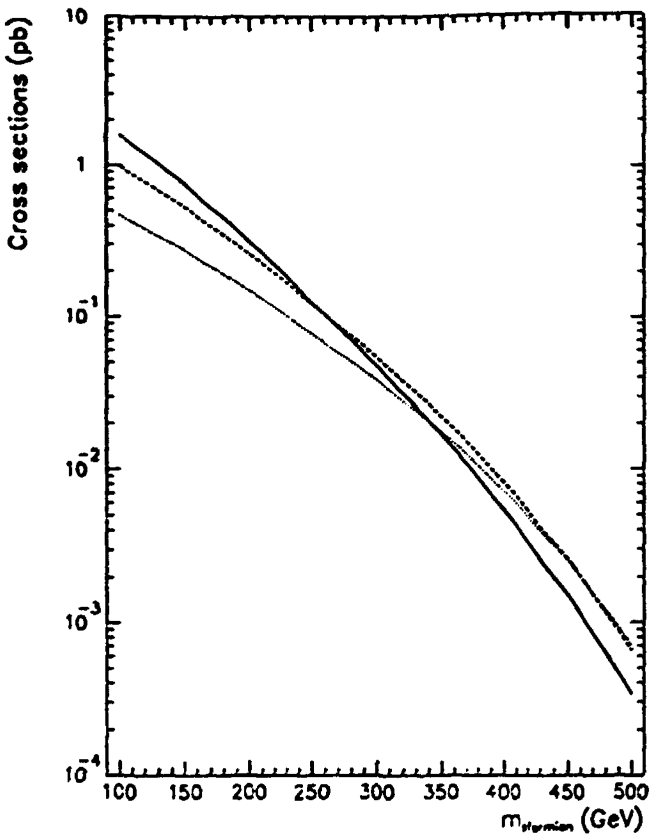

Fig. 20: Cross section for $e+p \to \tilde{e}+\tilde{q}+X$, summed over all left and right selectron and squark flavours, as a function of the sfermion mass taking $m_{\tilde{e}} = m_{\tilde{q}}$, for $\tan\beta = 4$, for $\mu = -200$ GeV and $M = 200$ GeV (——), 400 GeV (- - -), 800 GeV (· · · ·)..

Missing momentum as well as Z^0's and multileptons in the final state serve as good signatures. If LEP/LHC will also be operated in the ep collider mode, then it will be possible to cover a mass range for selectrons and sneutrinos according to $m_{\tilde{e},\tilde{\nu}} + m_{\tilde{q}} \leq 600$ GeV. A linear e^+e^- collider with c.m. energy of several hundred GeV up to 2 TeV would offer the unique possibility of exploring the properties of the non-strongly supersymmetric particles. We have studied in detail supersymmetric particle production at a 500 GeV e^+e^- collider. Such a collider would allow us to rule out the Minimal Supersymmetric Standard Model if no Higgs particle will be found. Moreover, it would extend the mass range of charged supersymmetric particles up to almost 250 GeV.

Concerning the explorable SUSY parameter range, a 500 GeV e^+e^- collider is roughly comparable to the LHC. Whereas at the LHC the strongly interacting SUSY particles up to a high mass can be detected, an e^+e^- collider is best suited for a detailed study of the non-strongly interacting SUSY particles. This would be necessary for fixing the SUSY model and its parameters.

A Appendix

A.1 Chargino and neutralino mixing

The chargino mass matrix as defined in [2, 4] is diagonalized by two unitary 2×2 matrices U and V,

$$\chi_i^+ = V_{ij}\psi_j^+, \qquad \chi_i^- = U_{ij}\psi_j^-, \qquad i = 1,2 \tag{A.1}$$

where

$$\psi_j^+ = (-i\lambda^+, \psi_{H_2}^1), \qquad \psi_j^- = (-i\lambda^-, \psi_{H_1}^2) \tag{A.2}$$

with $\lambda^\pm$, and $\psi_{H_2}^1$, $\psi_{H_1}^2$ the two-component spinors of the $W^\pm$-ino, and the charged higgsinos $\tilde{H}_1^+$, $\tilde{H}_2^-$, respectively. The two-component spinors χ_i^+ and χ_i^- are combined to the four-component Dirac spinors of the charginos:

$$\tilde{\chi}_i^+ = \begin{pmatrix} \chi_i^+ \\ \bar{\chi}_i^- \end{pmatrix} \qquad i = 1,2. \tag{A.3}$$

Explicit formulae for the elements of U and V can be found in [15].

The 4×4 neutralino mass matrix as defined in [2, 4] is diagonalized by the 4×4 unitary matrix N,

$$\chi_i^0 = N_{ij}\psi_j^0 \qquad j = 1,4 \tag{A.4}$$

in the basis

$$\psi_j^0 = (-i\lambda_\gamma, -i\lambda_Z, \psi_{H_1}^1 \cos\beta - \psi_{H_2}^2 \sin\beta, \psi_{H_1}^1 \sin\beta + \psi_{H_2}^2 \cos\beta) \tag{A.5}$$

with λ_γ, λ_Z, $\psi_{H_1}^1$ and $\psi_{H_2}^2$ denoting the two-component spinor-fields of the photino, Z-ino, and the neutral higgsinos, respectively. The four-component Majorana spinors of the neutralinos $\tilde{\chi}_i^0$ are then constructed from the two-component spinors χ_i^0.

A.2 Chargino production

The cross section for $e^+e^- \to \tilde{\chi}_i^+\tilde{\chi}_j^-$ is given by [40]:

$$\frac{d\sigma}{dt} = \frac{d\sigma_\gamma}{dt} + \frac{d\sigma_Z}{dt} + \frac{d\sigma_{\tilde{\nu}}}{dt} + \frac{d\sigma_{\gamma Z}}{dt} + \frac{d\sigma_{\gamma\tilde{\nu}}}{dt} + \frac{d\sigma_{Z\tilde{\nu}}}{dt} \tag{A.6}$$

$$\frac{d\sigma_\gamma}{dt} = \frac{e^4}{8\pi s^4}\delta_{ij}\left((M_i^2 - u)(M_j^2 - u) + (M_i^2 - t)(M_j^2 - t) + 2M_iM_js\right) \tag{A.7}$$

$$\begin{aligned}\frac{d\sigma_Z}{dt} = {} & \frac{g^4|D_Z(s)|^2}{32\pi s^2\cos^4\theta_W}\Big((L_e^2 + R_e^2)((O'^L_{ij})^2 + (O'^R_{ij})^2) \\ & \left[(M_i^2 - u)(M_j^2 - u) + (M_i^2 - t)(M_j^2 - t)\right] + \\ & 4(L_e^2 + R_e^2)O'^L_{ij}O'^R_{ij}\eta_i\eta_jM_iM_js - (L_e^2 - R_e^2)((O'^L_{ij})^2 - (O'^R_{ij})^2) \\ & \left[(M_i^2 - u)(M_j^2 - u) - (M_i^2 - t)(M_j^2 - t)\right]\Big)\end{aligned} \tag{A.8}$$

$$\frac{d\sigma_{\tilde{\nu}}}{dt} = \frac{g^4|D_{\tilde{\nu}}(t)|^2}{64\pi s^2}(V_{i1})^2(V_{j1})^2(M_i^2 - t)(M_j^2 - t) \tag{A.9}$$

$$\begin{aligned}\frac{d\sigma_{\gamma Z}}{dt} = {} & \frac{e^2g^2\,\mathrm{Re}(D_Z(s))}{16\pi s^3\cos^2\theta_W}\delta_{ij}\Big((L_e + R_e)(O'^L_{ij} + O'^R_{ij}) \\ & \left[(M_i^2 - u)(M_j^2 - u) + (M_i^2 - t)(M_j^2 - t) + 2M_iM_js\right] - \\ & (L_e - R_e)(O'^L_{ij} - O'^R_{ij})\left[(M_i^2 - u)(M_j^2 - u) - (M_i^2 - t)(M_j^2 - t)\right]\Big)\end{aligned} \tag{A.10}$$

channel	$\tilde{q}_H \bar{\tilde{q}}_K$		
s	γ, Z		
coeff.	LL	LR	RR
A_γ^{HK}	$\frac{3e^4 e_q^2}{8\pi}$	–	$\frac{3e^4 e_q^2}{8\pi}$
A_Z^{HK}	$\frac{3g^4 L_q^2(L_e^2+R_e^2)}{16\pi\cos^4\theta_W}$	–	$\frac{3g^4 R_q^2(L_e^2+R_e^2)}{16\pi\cos^4\theta_W}$
$A_{\gamma Z}^{HK}$	$\frac{3e^2 e_q g^2 L_q(L_e+R_e)}{8\pi\cos^2\theta_W}$	–	$\frac{3e^2 e_q g^2 R_q(L_e+R_e)}{8\pi\cos^2\theta_W}$

Tab. 1: The coefficients as appearing in eqs. (A.18 - A.23) for the cross section $e^+e^- \to \tilde{q}_H \bar{\tilde{q}}_K$. Here $e = g\sin\theta_W$, $e > 0$, and e_q is the charge of the quark in units of e. The couplings are given in Appendix A.6. Notice that $A_{\tilde{\chi}}^{HK} = B_{\tilde{\chi}}^{HK} = A_{\gamma\tilde{\chi}}^{HK} = A_{Z\tilde{\chi}}^{HK} = 0$.

$$\frac{d\sigma_{\gamma\tilde{\nu}}}{dt} = \frac{e^2 g^2 D_{\tilde{\nu}}(t)(V_{i1})^2}{16\pi s^3}\delta_{ij}\left((M_i^2 - t)(M_j^2 - t) + M_i M_j s\right) \tag{A.11}$$

$$\begin{aligned}\frac{d\sigma_{Z\tilde{\nu}}}{dt} &= \frac{g^4 \operatorname{Re}(D_{\tilde{\nu}}(t)D_Z^*(s))}{16\pi s^2\cos^2\theta_W} L_e V_{i1} V_{j1} \\ &\left[O_{ij}'^L(M_i^2 - t)(M_j^2 - t) + O_{ij}'^R \eta_i\eta_j M_i M_j s\right]\end{aligned} \tag{A.12}$$

where $D_Z = (s - m_Z^2 + im_Z\Gamma_Z)^{-1}$, $D_{\tilde{\nu}} = (t - m_{\tilde{\nu}}^2)^{-1}$. M_i is the (positive valued) mass of the chargino $\tilde{\chi}_i^\pm$, and $\eta_i = \pm 1$ is the sign of the corresponding mass eigenvalue. The couplings L_e, R_e, $O_{ij}'^{L,R}$ are given in Appendix A.6.

A.3 Neutralino production

The cross section for $e^+e^- \to \tilde{\chi}_i^0\tilde{\chi}_j^0$ is given by [40]:

$$\frac{d\sigma}{dt} = \frac{d\sigma_Z}{dt} + \frac{d\sigma_{\tilde{e}}}{dt} + \frac{d\sigma_{Z\tilde{e}}}{dt} \tag{A.13}$$

$$\begin{aligned}\frac{d\sigma_Z}{dt} &= \frac{g^4}{16\pi s^2\cos^4\theta_W}|D_Z(s)|^2(O_{ij}''^L)^2(L_e^2 + R_e^2) \\ &\left[(m_i^2 - u)(m_j^2 - u) + (m_i^2 - t)(m_j^2 - t) - 2\eta_i\eta_j m_i m_j s\right]\end{aligned} \tag{A.14}$$

$$\begin{aligned}\frac{d\sigma_{\tilde{e}}}{dt} &= \frac{g^4}{64\pi s^2}\Bigg\{\left(f_{ei}^L f_{ej}^L\right)^2\Big[|D_{\tilde{e}_L}(t)|^2(m_i^2 - t)(m_j^2 - t) + \\ &|D_{\tilde{e}_L}(u)|^2(m_i^2 - u)(m_j^2 - u) - 2\operatorname{Re}(D_{\tilde{e}_L}(t)D_{\tilde{e}_L}^*(u))\eta_i\eta_j m_i m_j s\Big] + \\ &\left(f_{ei}^R f_{ej}^R\right)^2\Big[|D_{\tilde{e}_R}(t)|^2(m_i^2 - t)(m_j^2 - t) +\end{aligned}$$

$$|D_{\tilde{e}_R}(u)|^2(m_i^2-u)(m_j^2-u) - 2\,\mathrm{Re}(D_{\tilde{e}_R}(t)D^*_{\tilde{e}_R}(u))\eta_i\eta_j m_i m_j s\Big]\Big\} \quad (A.15)$$

$$\begin{aligned}
\frac{d\sigma_{Z\tilde{e}}}{dt} &= \frac{g^4}{16\pi s^2\cos^2\theta_W}\mathrm{Re}(D_Z(s))O''^{L}_{ij} \\
&\Big\{L_e f^L_{ei} f^L_{ej}\Big[D_{\tilde{e}_L}(t)\left((m_i^2-t)(m_j^2-t)-\eta_i\eta_j m_i m_j s\right) + \\
&D_{\tilde{e}_L}(u)\left((m_i^2-u)(m_j^2-u)-\eta_i\eta_j m_i m_j s\right)\Big] - \\
&R_e f^R_{ei} f^R_{ej}\Big[D_{\tilde{e}_R}(t)\left((m_i^2-t)(m_j^2-t)-\eta_i\eta_j m_i m_j s\right) + \\
&D_{\tilde{e}_R}(u)\left((m_i^2-u)(m_j^2-u)-\eta_i\eta_j m_i m_j s\right)\Big]\Big\}, \qquad (A.16)
\end{aligned}$$

where $D_Z = (s - m_Z^2 + i m_Z\Gamma_Z)^{-1}$, $D_{\tilde{e}_{L,R}}(x) = (x - m^2_{\tilde{e}_{L,R}})^{-1}$. m_i is the (positive valued) mass of the neutralino $\tilde{\chi}^0_i$, and $\eta_i = \pm 1$ is the sign of the corresponding mass eigenvalue. The couplings $O''^{L,R}_{ij}$, $f^{L,R}_{ei}$ are given in Appendix A.6.

A.4 Sfermionproduction

The cross section for $e^+e^- \to \tilde{f}_H\bar{\tilde{f}}_K$, where $\tilde{f}$ is a slepton or a squark (H, $K = L$ or R), is given by [40]:

$$\frac{d\sigma}{dt} = \frac{d\sigma_\gamma}{dt} + \frac{d\sigma_Z}{dt} + \frac{d\sigma_{\tilde{\chi}}}{dt} + \frac{d\sigma_{\gamma Z}}{dt} + \frac{d\sigma_{\gamma\tilde{\chi}}}{dt} + \frac{d\sigma_{Z\tilde{\chi}}}{dt}, \qquad (A.17)$$

$$\begin{aligned}
\frac{d\sigma_\gamma}{dt} &= A^{HK}_\gamma \frac{\left(ut - M^2_{\tilde{f}_H}M^2_{\tilde{f}_K}\right)}{s^4} && (A.18)\\
\frac{d\sigma_Z}{dt} &= A^{HK}_Z \frac{\left(ut - M^2_{\tilde{f}_H}M^2_{\tilde{f}_K}\right)}{s^2}|D_Z(s)|^2 && (A.19)\\
\frac{d\sigma_{\tilde{\chi}}}{dt} &= \frac{\left(ut - M^2_{\tilde{f}_H}M^2_{\tilde{f}_K}\right)}{s^2}\left(\sum_i A^{HK}_{\tilde{\chi}} D_i(t)\right)^2 + \\
&\sum_{i,j}\frac{\eta_i\eta_j m_i m_j B^{HK}_{\tilde{\chi}} D_i(t) D_j(t)}{s} && (A.20)\\
\frac{d\sigma_{\gamma Z}}{dt} &= A^{HK}_{\gamma Z}\frac{\left(ut - M^2_{\tilde{f}_H}M^2_{\tilde{f}_K}\right)}{s^3}\mathrm{Re}(D_Z(s)) && (A.21)\\
\frac{d\sigma_{\gamma\tilde{\chi}}}{dt} &= \frac{\left(ut - M^2_{\tilde{f}_H}M^2_{\tilde{f}_K}\right)}{s^3}\sum_i A^{HK}_{\gamma\tilde{\chi}} D_i(t) && (A.22)\\
\frac{d\sigma_{Z\tilde{\chi}}}{dt} &= \frac{\left(ut - M^2_{\tilde{f}_H}M^2_{\tilde{f}_K}\right)}{s^2}\mathrm{Re}(D_Z(s))\sum_i A^{HK}_{Z\tilde{\chi}} D_i(t), && (A.23)
\end{aligned}$$

where $D_Z = (s - m_Z^2 + i m_Z\Gamma_Z)^{-1}$, $D_i(t) = (t - m_i^2)^{-1}$. m_i is the (positive valued) mass of the exchanged neutralino $\tilde{\chi}^0_i$ or chargino $\tilde{\chi}^\pm_i$, and $\eta_i = \pm 1$ is the sign of the corresponding

channel	$\tilde{e}^+_H \tilde{e}^-_K$			$\tilde{\nu}_e \bar{\tilde{\nu}}_e$
s	γ, Z			Z
t	$\tilde{\chi}^0_i$			$\tilde{\chi}^\pm_i$
coeff.	LL	LR	RR	LL
A^{HK}_γ	$\frac{e^4}{8\pi}$	–	$\frac{e^4}{8\pi}$	–
A^{HK}_Z	$\frac{g^4 L_e^2(L_e^2+R_e^2)}{16\pi\cos^4\theta_W}$	–	$\frac{g^4 R_e^2(L_e^2+R_e^2)}{16\pi\cos^4\theta_W}$	$\frac{g^4(L_e^2+R_e^2)}{64\pi\cos^4\theta_W}$
$A^{HK}_{\tilde{\chi}}$	$\frac{g^2\lvert f^L_{ei}\rvert^2}{8\sqrt{\pi}}$	–	$\frac{g^2\lvert f^R_{ei}\rvert^2}{8\sqrt{\pi}}$	$\frac{g^2(V_{i1})^2}{8\sqrt{\pi}}$
$B^{HK}_{\tilde{\chi}}$	–	$\frac{g^4}{64\pi} f^R_{ei} f^L_{ei} f^R_{ej} f^L_{ej}$	–	–
$A^{HK}_{\gamma Z}$	$\frac{e^2 g^2 L_e(L_e+R_e)}{8\pi\cos^2\theta_W}$	–	$\frac{e^2 g^2 R_e(L_e+R_e)}{8\pi\cos^2\theta_W}$	–
$A^{HK}_{\gamma\tilde{\chi}}$	$\frac{e^2 g^2\lvert f^L_{ei}\rvert^2}{16\pi}$	–	$\frac{e^2 g^2\lvert f^R_{ei}\rvert^2}{16\pi}$	–
$A^{HK}_{Z\tilde{\chi}}$	$\frac{g^4 L_e^2\lvert f^L_{ei}\rvert^2}{16\pi\cos^2\theta_W}$	–	$\frac{g^4 R_e^2\lvert f^R_{ei}\rvert^2}{16\pi\cos^2\theta_W}$	$\frac{g^4 L_e(V_{i1})^2}{32\pi\cos^2\theta_W}$
channel	$\tilde{l}^+_H \tilde{l}^-_K,\ \tilde{l} = \tilde{\mu}, \tilde{\tau}$			$\tilde{\nu}_l \bar{\tilde{\nu}}_l$
s	γ, Z			Z
t	–			–
coeff.	LL	LR	RR	LL
A^{HK}_γ	$\frac{e^4}{8\pi}$	–	$\frac{e^4}{8\pi}$	–
A^{HK}_Z	$\frac{g^4 L_l^2(L_e^2+R_e^2)}{16\pi\cos^4\theta_W}$	–	$\frac{g^4 R_l^2(L_e^2+R_e^2)}{16\pi\cos^4\theta_W}$	$\frac{g^4(L_e^2+R_e^2)}{64\pi\cos^4\theta_W}$
$A^{HK}_{\tilde{\chi}}$	–	–	–	–
$B^{HK}_{\tilde{\chi}}$	–	–	–	–
$A^{HK}_{\gamma Z}$	$\frac{e^2 g^2 L_l(L_e+R_e)}{8\pi\cos^2\theta_W}$	–	$\frac{e^2 g^2 R_l(L_e+R_e)}{8\pi\cos^2\theta_W}$	–
$A^{HK}_{\gamma\tilde{\chi}}$	–	–	–	–
$A^{HK}_{Z\tilde{\chi}}$	–	–	–	–

Tab. 2: The coefficients as appearing in eqs. (A.18 - A.23) for the cross section $e^+e^- \to \tilde{f}_H \bar{\tilde{f}}_K$, $\tilde{f} = \tilde{e}, \tilde{\mu}, \tilde{\tau}, \tilde{\nu}_e, \tilde{\nu}_\mu, \tilde{\nu}_\tau$. The couplings are given in Appendix A.6.

$\tilde{\chi}_i^+ \to$	$\tilde{\chi}_k^0 u\bar{d}$	$\tilde{\chi}_k^+ u\bar{u}$	$\tilde{\chi}_k^+ d\bar{d}$
A_s	$6\,(O_{ki}^L)^2$	$12\,\frac{(L_u O'^L_{ki})^2+(R_u O'^R_{ki})^2}{\cos^4\theta_W}$	$12\,\frac{(L_d O'^L_{ki})^2+(R_d O'^R_{ki})^2}{\cos^4\theta_W}$
B_s	$6\,(O_{ki}^R)^2$	$12\,\frac{(L_u O'^R_{ki})^2+(R_u O'^L_{ki})^2}{\cos^4\theta_W}$	$12\,\frac{(L_d O'^R_{ki})^2+(R_d O'^L_{ki})^2}{\cos^4\theta_W}$
C_s	$-6\,O_{ki}^L O_{ki}^R$	$-12\,\frac{(L_u^2+R_u^2)O'^L_{ki}O'^R_{ki}}{\cos^4\theta_W}$	$-12\,\frac{(L_d^2+R_d^2)O'^L_{ki}O'^R_{ki}}{\cos^4\theta_W}$
A_t^L	$3\,(f_{uk}^L V_{i1})^2$	0	$3\,(V_{k1}V_{i1})^2$
A_u^L	$3\,(f_{dk}^L U_{i1})^2$	$3\,(U_{k1}U_{i1})^2$	0
A_{tu}^L	$3\,f_{uk}^L f_{dk}^L V_{i1} U_{i1}$	0	0
A_{st}^L	$-3\sqrt{2} f_{uk}^L V_{i1} O_{ki}^L$	0	$6\,\frac{V_{k1}V_{i1}O'^L_{ki}L_d}{\cos^2\theta_W}$
B_{st}^L	$3\sqrt{2} f_{uk}^L V_{i1} O_{ki}^R$	0	$-6\,\frac{V_{k1}V_{i1}O'^R_{ki}L_d}{\cos^2\theta_W}$
A_{su}^L	$3\sqrt{2} f_{dk}^L U_{i1} O_{ki}^R$	$-6\,\frac{U_{k1}U_{i1}O'^R_{ki}L_u}{\cos^2\theta_W}$	0
B_{su}^L	$-3\sqrt{2} f_{dk}^L U_{i1} O_{ki}^L$	$6\,\frac{U_{k1}U_{i1}O'^L_{ki}L_u}{\cos^2\theta_W}$	0

Tab. 3: Coefficients in eqs. (A.25 – A.30) for hadronic chargino decays. The couplings are given in the Appendix A.6. Notice that $A_t^R = A_u^R = A_{ut}^R = A_{st}^R = A_{su}^R = B_{st}^R = B_{su}^R = 0$.

mass eigenvalue. $M_{\tilde{f}_H}$ is the mass of the produced sfermion $\tilde{f}_H$. Here $m_f = 0$ has been taken for the corresponding fermion f. The coefficients $A_\gamma^{H,K}$, $A_Z^{H,K}$ etc. are given in Tab. 1 and 2.

A.5 Three-body decay

The width for the decay of a chargino or neutralino into a lighter chargino or neutralino and a fermion pair is given by [34]:

$$\Gamma(\tilde{\chi}_i \to \tilde{\chi}_k + f\bar{f}') = \frac{\alpha^2}{32\pi \sin^4\theta_W m_i^3} \int d\bar{s}\, d\bar{t}\, (W_s + W_t + W_u + W_{tu} + W_{st} + W_{su}) \quad \text{(A.24)}$$

$$\begin{aligned} W_s &= \frac{1}{(\bar{s} - M_s^2)^2}\Big(A_s(m_i^2 - \bar{t})(\bar{t} - m_k^2) + \\ &\qquad B_s(m_i^2 - \bar{u})(\bar{u} - m_k^2) + 2\,C_s \eta_i \eta_k m_i m_k \bar{s}\Big) &\text{(A.25)} \\ W_t &= A_t^L \frac{(m_i^2 - \bar{t})(\bar{t} - m_k^2)}{(\bar{t} - M_L^2)^2} + A_t^R \frac{(m_i^2 - \bar{t})(\bar{t} - m_k^2)}{(\bar{t} - M_R^2)^2} &\text{(A.26)} \\ W_u &= A_u^L \frac{(m_i^2 - \bar{u})(\bar{u} - m_k^2)}{(\bar{u} - M_L^2)^2} + A_u^R \frac{(m_i^2 - \bar{u})(\bar{u} - m_k^2)}{(\bar{u} - M_R^2)^2} &\text{(A.27)} \end{aligned}$$

$\tilde{\chi}_i^+ \to$	$\tilde{\chi}_k^0 l^+ \nu$	$\tilde{\chi}_k^+ l^+ l^-$	$\tilde{\chi}_k^+ \nu \bar{\nu}$
A_s	$2(O_{ki}^L)^2$	$4\,\frac{(L_l O'^L_{ki})^2+(R_l O'^R_{ki})^2}{\cos^4\theta_W}$	$\frac{(O'^L_{ki})^2}{\cos^4\theta_W}$
B_s	$2(O_{ki}^R)^2$	$4\,\frac{(L_l O'^R_{ki})^2+(R_l O'^L_{ki})^2}{\cos^4\theta_W}$	$\frac{(O'^R_{ki})^2}{\cos^4\theta_W}$
C_s	$-2O_{ki}^L O_{ki}^R$	$-4\,\frac{(L_l^2+R_l^2)O'^L_{ki}O'^R_{ki}}{\cos^4\theta_W}$	$-\frac{O'^L_{ki}O'^R_{ki}}{\cos^4\theta_W}$
A_t^L	$(f_{\nu k}^L V_{i1})^2$	$(V_{k1}V_{i1})^2$	0
A_u^L	$(f_{lk}^L U_{i1})^2$	0	$(U_{k1}U_{i1})^2$
A_{tu}^L	$f_{\nu k}^L f_{dk}^L V_{i1} U_{i1}$	0	0
A_{st}^L	$-\sqrt{2} f_{\nu k}^L V_{i1} O_{ki}^L$	$2\,\frac{V_{k1}V_{i1}O'^L_{ki}L_l}{\cos^2\theta_W}$	0
B_{st}^L	$\sqrt{2} f_{\nu k}^L V_{i1} O_{ki}^R$	$-2\,\frac{V_{k1}V_{i1}O'^R_{ki}L_l}{\cos^2\theta_W}$	0
A_{su}^L	$\sqrt{2} f_{lk}^L U_{i1} O_{ki}^R$	0	$-\frac{U_{k1}U_{i1}O'^R_{ki}}{\cos^2\theta_W}$
B_{su}^L	$-\sqrt{2} f_{lk}^L U_{i1} O_{ki}^L$	0	$\frac{U_{k1}U_{i1}O'^L_{ki}}{\cos^2\theta_W}$

Tab. 4: Coefficients in eqs. (A.25 - A.30) for leptonic chargino decays. The couplings are given in the Appendix A.6. Notice that $A_t^R = A_u^R = A_{ut}^R = A_{st}^R = A_{su}^R = B_{st}^R = B_{su}^R = 0$.

$$
\begin{aligned}
W_{tu} &= A_{tu}^L \frac{2\eta_i\eta_k m_i m_k \bar{s}}{(\bar{t}-M_L^2)(\bar{u}-M_L^2)} + A_{tu}^R \frac{2\eta_i\eta_k m_i m_k \bar{s}}{(\bar{t}-M_R^2)(\bar{u}-M_R^2)} && \text{(A.28)}\\
W_{st} &= \frac{2}{(\bar{t}-M_L^2)(\bar{s}-M_s^2)}\left(A_{st}^L(m_i^2-\bar{t})(\bar{t}-m_k^2) + B_{st}^L\eta_i\eta_k m_i m_k \bar{s}\right) + \\
&\quad (L \leftrightarrow R) && \text{(A.29)}\\
W_{su} &= \frac{2}{(\bar{u}-M_L^2)(\bar{s}-M_s^2)}\left(A_{su}^L(m_i^2-\bar{u})(\bar{u}-m_k^2) + B_{su}^L\eta_i\eta_k m_i m_k \bar{s}\right) + \\
&\quad (L \leftrightarrow R). && \text{(A.30)}
\end{aligned}
$$

m_i is the (positive valued) mass of the chargino or neutralino $\tilde{\chi}_i$, and $\eta_i = \pm 1$ is the sign of the corresponding mass eigenvalue. M_s is the mass of the $W^\pm$, Z, exchanged in the $\bar{s}$ channel. M_L, M_R denote the masses of the left and right sfermion exchanged in the $\bar{t}$- and $\bar{u}$ channel. The range of integration for $\bar{s}$ and $\bar{t}$ is given by the bounds, $\bar{s}_{min} = 0$, $\bar{s}_{max} = (m_i - m_k)^2$, $\bar{t}_{min,max} = 1/2(m_i^2 + m_k^2 - \bar{s} \mp \sqrt{\lambda(m_i^2, m_k^2, \bar{s})})$, $\lambda(a,b,c) = a^2 + b^2 + c^2 - 2ab - 2bc - 2ca$. The coefficients A_s, B_s, etc. are given in Tab. 3 - 6.

A.6 Couplings

$$
f_{fk}^L = -\sqrt{2}\left[\frac{1}{\cos\theta_W}\left(T_{3f} - e_f \sin^2\theta_W\right) N_{k2} + e_f \sin\theta_W N_{k1}\right] \qquad \text{(A.31)}
$$

$\tilde{\chi}_i^0 \to$	$\tilde{\chi}_k^0 l^+ l^-$	$\tilde{\chi}_k^0 \nu\bar{\nu}$	$\tilde{\chi}_k^0 q\bar{q}$
$A_s = B_s = C_s$	$4\,\frac{(O''^L_{ki})^2(L_l^2+R_l^2)}{\cos^4\theta_W}$	$\frac{(O''^L_{ki})^2}{\cos^4\theta_W}$	$12\,\frac{(O''^L_{ki})^2(L_q^2+R_q^2)}{\cos^4\theta_W}$
$A_t^L = A_u^L = A_{tu}^L$	$(f_{lk}^L f_{li}^L)^2$	$(f_{\nu k}^L f_{\nu i}^L)^2$	$3\,(f_{qk}^L f_{qi}^L)^2$
$A_t^R = A_u^R = A_{tu}^R$	$(f_{lk}^R f_{li}^R)^2$	0	$3\,(f_{qk}^R f_{qi}^R)^2$
$A_{st}^L = B_{st}^L = A_{su}^L = B_{su}^L$	$2\,\frac{f_{lk}^L f_{li}^L O''^L_{ki} L_l}{\cos^2\theta_W}$	$\frac{f_{\nu k}^L f_{\nu i}^L O''^L_{ki}}{\cos^2\theta_W}$	$6\,\frac{f_{qk}^L f_{qi}^L O''^L_{ki} L_q}{\cos^2\theta_W}$
$A_{st}^R = B_{st}^R = A_{su}^R = B_{su}^R$	$2\,\frac{f_{lk}^R f_{li}^R O''^R_{ki} R_l}{\cos^2\theta_W}$	0	$6\,\frac{f_{qk}^R f_{qi}^R O''^R_{ki} R_q}{\cos^2\theta_W}$

Tab. 5: Coefficients in eqs. (A.25 – A.30) for $\tilde{\chi}_i^0 \to \tilde{\chi}_k^0 f\bar{f}$. The couplings are given in the Appendix A.6.

$\tilde{\chi}_i^0 \to$	$\tilde{\chi}_k^+ l^- \bar{\nu}$	$\tilde{\chi}_k^+ \bar{u} d$
A_s	$2\,(O_{ik}^L)^2$	$6\,(O_{ik}^L)^2$
B_s	$2\,(O_{ik}^R)^2$	$6\,(O_{ik}^R)^2$
C_s	$-2\,O_{ik}^L O_{ik}^R$	$-6\,O_{ik}^L O_{ik}^R$
A_t^L	$(f_{\nu i}^L V_{k1})^2$	$3\,(f_{ui}^L V_{k1})^2$
A_u^L	$(f_{li}^L U_{k1})^2$	$3\,(f_{di}^L U_{k1})^2$
A_{tu}^L	$f_{\nu i}^L f_{li}^L V_{k1} U_{k1}$	$3\,f_{ui}^L f_{di}^L V_{k1} U_{k1}$
A_{st}^L	$-\sqrt{2} f_{\nu i}^L V_{k1} O_{ik}^L$	$-3\sqrt{2} f_{ui}^L V_{k1} O_{ik}^L$
B_{st}^L	$\sqrt{2} f_{\nu i}^L V_{k1} O_{ik}^R$	$3\sqrt{2} f_{ui}^L V_{k1} O_{ik}^R$
A_{su}^L	$\sqrt{2} f_{li}^L U_{k1} O_{ik}^R$	$3\sqrt{2} f_{di}^L U_{k1} O_{ik}^R$
B_{su}^L	$-\sqrt{2} f_{li}^L U_{k1} O_{ik}^L$	$-3\sqrt{2} f_{di}^L U_{k1} O_{ik}^L$

Tab. 6: Coefficients in eqs. (A.25 – A.30) for $\tilde{\chi}_i^0 \to \tilde{\chi}_k^+ f\bar{f}'$. The couplings are given in the Appendix A.6. Notice that $A_t^R = A_u^R = A_{ut}^R = A_{st}^R = A_{su}^R = B_{st}^R = B_{su}^R = 0$.

$$f^R_{fk} = -\sqrt{2}e_f \sin\theta_W (\tan\theta_W N_{k2} - N_{k1}) \tag{A.32}$$
$$L_f = T_{3f} - e_f \sin^2\theta_W \tag{A.33}$$
$$R_f = -e_f \sin^2\theta_W \tag{A.34}$$
$$O^L_{ij} = -(N_{i4}\cos\beta - N_{i3}\sin\beta)\frac{V_{j2}}{\sqrt{2}} + (N_{i1}\sin\theta_W + N_{i2}\cos\theta_W)V_{j1} \tag{A.35}$$
$$O^R_{ij} = (N_{i4}\sin\beta + N_{i3}\cos\beta)\frac{U_{j2}}{\sqrt{2}} + (N_{i1}\sin\theta_W + N_{i2}\cos\theta_W)U_{j1} \tag{A.36}$$
$$O'^{\,L}_{ij} = -V_{i1}V_{j1} - \frac{1}{2}V_{i2}V_{j2} + \delta_{ij}\sin^2\theta_W \tag{A.37}$$
$$O'^{\,R}_{ij} = -U_{i1}U_{j1} - \frac{1}{2}U_{i2}U_{j2} + \delta_{ij}\sin^2\theta_W \tag{A.38}$$
$$\begin{aligned} O''^{\,L}_{ij} &= -\frac{1}{2}(N_{i3}\cos\beta + N_{i4}\sin\beta)(N_{j3}\cos\beta + N_{j4}\sin\beta) \\ &\quad +\frac{1}{2}(-N_{i3}\sin\beta + N_{i4}\cos\beta)(-N_{j3}\sin\beta + N_{j4}\cos\beta) \end{aligned} \tag{A.39}$$
$$O''^{\,R}_{ij} = -O''^{\,L}_{ij}. \tag{A.40}$$

Here T_{3f} and e_f are the third component of weak isospin and the charge (in units of e) of the fermion f. We have used a convention where the matrices U, V, and N are real.

References

[1] For a general introduction to supersymmetry, see J. Wess, J. Bagger, Supersymmetry and Supergravity, Princeton University Press, 1983

[2] H.-P. Nilles, these Lecture Notes

[3] H.P. Nilles, Phys. Rep. 110 (1984) 1; B. Lahanas, D.V. Nanopoulos, Phys. Rep. 145 (1985) 1; R. Barbieri, Riv. Nuov. Cim. 11 (1988) 1

[4] H.E. Haber, G.L. Kane, Phys. Rep. 117 (1985)

[5] L.J. Hall, J. Polchinski, Phys. Lett. 152B (1985) 335

[6] J.F. Gunion, H.E. Haber, Nucl. Phys. B272 (1986) 1; J.F. Gunion, H.E. Haber, G.L. Kane, S. Dawson, "The Higgs Hunter's Guide", Addison-Wesley, 1990

[7] G. Ridolfi, Joint Int. Lepton-Photon Symposium and Europhysics Conference on High Energy Physics, Geneva, 1991, and references therein, to appear

[8] J. Kalinowski, these Lecture Notes, and references therein;
S. Pokorski, these Lecture Notes

[9] M. Davier, Proceedings of the Joint Int. Lepton-Photon Symp. and Europhysics Conf. on High Energy Physics, Geneva, 1991

[10] H. Baer, X. Tata, J. Woodside, Phys. Rev. D44 (1991) 207

[11] H. Baer et al., FSU-HE-910308, BU/TH/91-1, UCD-91-4, UH-511-922-91

[12] H. Baer, A. Bartl, D. Karatas, W. Majerotto, X. Tata, Int. J. of Mod. Phys. A4 (1989) 4111

[13] J.F. Gunion, H.E. Haber, Phys. Rev. D37 (1988) 2515

[14] M. Chen, C. Dionisi, M. Martinez, X. Tata, Phys. Rep. 159 (1988) 201; C. Dionisi et al., Proc. of the ECFA Workshop on LEP 200, Aachen, 1986, Vol. II, p. 380, CERN 87 - 08, ECFA 878/108

[15] A. Bartl, H. Fraas, W. Majerotto, B. Mößlacher, preprint UWThPh-1991-44, HEPHY-PUB-561-91

[16] Proceedings of the Workshop on Physics and Experiments with Linear Colliders, Lapland, Finland, 1991, to appear

[17] Proceedings of the Workshop on e^+e^- Collisions at 500 GeV: The Physics Potential, DESY, Hamburg, 1991, to appear

[18] A. Brignole et. al., in [17]; P. Janot, in [17]

[19] A. Bartl, W. Majerotto, B. Mößlacher, in [17]

[20] J.F. Grivaz, in [17]

[21] A. Bartl, H. Fraas, W. Majerotto, N. Oshimo, Phys. Rev. D40 (1989) 1594

[22] C. Vander Velde, in [17]

[23] R. Becker, R. Starosta, in [17]

[24] V. Angelopoulos et al., Proc. of the Workshop on Physics at Future Accelerators, La Thuile, 1987, Vol. I, p. 80, CERN 87-07; A. Savoy-Navarro, N. Zaganidis, ibidem, Vol. II, p. 82; R. Batley, ibidem, Vol. II, p.109; H. Baer, X. Tata and J. Woodside, Proc. of the Summer Study on High Energy Physics in the 1990's, Snowmass, 1988, p. 220; R.M. Barnett et al., ibidem, p.226

[25] F. Pauss, Proc. of the ECFA Large Hadron Collider Workshop, Aachen, 1990, Vol. I, p. 118, CERN90-10, ECFA90-133

[26] S. Dawson, E. Eichten and C. Quigg, Phys. Rev. D31 (1985) 1581 and references therein

[27] Report of the Supersymmetry Working Group (Conveners: G.G. Ross and F. Zwirner), Proc. of the ECFA Large Hadron Collider Workshop, Aachen, 1990, Vol. II, CERN90-10, ECFA90-133

[28] A. Bartl, W. Majerotto, B. Mößlacher, N. Oshimo, S. Stippel, Phys. Rev. D43 (1991) 2214

[29] H. Baer, V. Barger, D. Karatas and X. Tata, Phys. Rev. D36 (1987) 96; R.M. Barnett, J.F. Gunion and H.E. Haber, Phys. Rev. Lett. 60 (1988) 401; Phys. Rev. D37 (1988) 1892

[30] H. Baer, X. Tata and J. Woodside, Phys. Rev. D42 (1990) 1568

[31] A. Bartl, W. Majerotto, B. Mößlacher, N. Oshimo, Z. Phys. C52 (1991) 477

[32] S.K. Jones and C.H. Llewellyn Smith, Nucl. Phys. B217 (1983) 145; P.R. Harrison, Nucl. Phys. B249 (1985) 704; J.A. Bagger and M.E. Peskin, Phys. Rev. D31 (1985) 2211; J. Bartels and W. Hollik, Z. Phys. C39 (1988) 433; T. Kon, K. Nakamura, T. Kobayashi, Z. Phys. C45 (1990) 567

[33] H. Komatsu and R. Rückl, Nucl. Phys. B299 (1988) 407; A. Bartl, H. Fraas and W. Majerotto, Nulc. Phys. B297 (1988) 479

[34] A. Bartl, H. Fraas and W. Majerotto, Z. Phys. C41 (1988) 475

[35] Proceedings of the HERA Workshop, DESY, Hamburg, 1991, to appear

[36] R. Rückl, Proc. of the ECFA Large Hadron Collider Workshop, Aachen, 1990, Vol. I, p. 229, CERN 90-10, ECFA 90-133

[37] A. Bartl, W. Majerotto, B. Mößlacher, N. Oshimo and S. Stippel, Proc. of the ECFA Large Hadron Collider Workshop, Aachen, 1990, Vol. II, p. 1033, CERN 90-10, ECFA 90-133

[38] A. Bartl, W. Majerotto, B. Mößlacher, N. Oshimo Z. Phys. C52 (1991) 677

[39] M. Besançon, Proc. of the ECFA Large Hadron Collider Workshop, Aachen, 1990, Vol. II, p. 1040, CERN 90-10, ECFA 90-133

[40] A. Bartl, H. Fraas, W. Majerotto, Z. Phys. C30 (1986) 441; Nucl. Phys. B278 (1986) 1; Z. Phys. C34 (1987) 411